



INDIAN INSTITUTE OF SCIENCE
EDUCATION AND RESEARCH MOHALI

MASTER'S THESIS

Extreme events in coupled Lotka Volterra systems

Author:
Abhijeet SINGH

Supervisor:
Prof. Sudeshna SINHA

*A thesis submitted in partial fulfillment of the requirements
for the degree of Bachelor and Master of Science (Dual Degree)*


in the

Department of Physical Sciences

May 26, 2021

Certificate of Examination

This is to certify that the dissertation titled **Extreme events in coupled Lotka Volterra systems** submitted by **Abhijeet Singh** (Reg. No. MS16129) for the partial fulfilment of BS-MS dual degree program of Indian Institute of Science Education and Research (IISER) Mohali, has been examined by the committee duly appointed by the Institute. The committee finds the work done by the candidate satisfactory and recommends that the report be accepted.



Prof. Sudeshna Sinha
(Supervisor)



Dr. Abhishek Chaudhuri
(Member of the Committee)



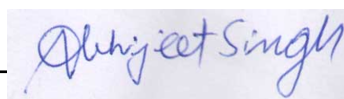
Dr. Dipanjan Chakraborty
(Member of the Committee)

Declaration of Authorship

I, Abhijeet SINGH, declare that this thesis titled, "Extreme events in coupled Lotka Volterra systems" and the work presented in it are my own. The work has been done at the Indian Institute of Science Education and Research Mohali under the guidance of Prof. Sudeshna Sinha.

This work has not been submitted in part or in full for a degree, a diploma, or a fellowship to any other university or institute. Whenever contributions of others are involved, every effort is made to indicate this clearly, with due acknowledgement of collaborative research and discussions. This thesis is a bonafide record of original work done by me and all sources listed within have been detailed in the bibliography.

Signed: _____



(Abhijeet Singh, Candidate)

Date: **23 May 2021**

In my capacity as the MS thesis supervisor of the candidate, I certify that the above statements by the candidate are true to the best of my knowledge.

Signed: _____



(Prof. Sudeshna Sinha, supervisor)

Date: **23 May 2021**

“Thanks to my solid academic training, today I can write hundreds of words on virtually any topic without possessing a shred of information, which is how I got a good job in journalism.”

Dave Barry

INDIAN INSTITUTE OF SCIENCE EDUCATION AND RESEARCH
MOHALI

Abstract

Department of Physical Sciences

Bachelor and Master of Science (Dual Degree)

Extreme events in coupled Lotka Volterra systems

by Abhijeet SINGH

We review the most important parts of a recent paper on the occurrence of extreme events in a generalized Lotka Volterra system, and reproduce the key results of the paper. We then extend the results to the occurrence of extreme events in a simple Lotka Volterra system. We study the characteristics of dynamics in the system that gives rise to extreme events in the simple Lotka Volterra system. We study the spatio-temporal occurrence of the extreme events. We also quantify the strength of the events as a function of coupling in the system. Further, we investigate the occurrence of extinction in the system for some special values of the coupling.

Acknowledgements

Like most other things in life, this work could not have been done without the help and support of a large number of people. Needless to say, the most important person in this pursuit was my supervisor, Prof. Sudeshna Sinha. She was a most helpful, patient and enthusiastic guide. I never felt pressurized to hurry through things. She also allowed me to have complete freedom in terms of what to pursue in the thesis. The discussions that I had with her formed the bedrock of what I did on my own.

I would also like to thank the other two committee members- Dr. Dipanjan Chakraborty and Dr. Abhishek Chaudhuri for showing interest in my work, and pitching in their suggestions. Many thanks are due to them for also keeping the campus of IISER Mohali functional for students in their officiating capacities as the deans, and providing us with all the facilities despite this being so difficult given the pandemic situation that was prevalent when the work was done. In the same breath I also thank Dr. Anu Sablok, former Dean (Students) of IISER Mohali and also the present and past wardens for putting in all the work they did for us.

I must also thank my friends Sasank and Mehak for listening to my ideas regarding the work, and also keeping me motivated towards working on it. I can't also forget the help that I received from them when I had sprained my foot and it was almost impossible for me to walk. Besides these two, I cannot forget Abhimanyu, Shikhar, Mohak, Ijaz, Vinod, Lakshita, Saurav, Anshul, BJ, Satender, Mayank- people who made my stay of nearly five years at IISER Mohali totally worth it.

It would be a shame if I don't thank my parents for everything I have received from them. Their constant encouragement has kept me going so far in my academic journey.

There are several other people who directly or indirectly helped me in working towards this thesis- a large number of friends, some faculty members etc. I cannot thank everyone individually here, but let it be said that I am extremely grateful to each and everyone of them.

I also thank the Stackoverflow community for answering my queries regarding coding various things in the Python language. I think the Stackexchange is one of the most wonderful things to have happened to the internet.

Lastly, I must thank the Librarian of IISER Mohali and the other members of the Library staff. Most of the work was done while in the library. They did a fantastic job of keeping the library running amidst the pandemic.

Contents

Declaration of Authorship	v
Abstract	ix
Acknowledgements	xi
Contents	xiii
List of Figures	xv
1 Advent of extreme events in Lotka Volterra systems	1
1.1 Introduction	1
1.2 Emergence of extreme events in an ecological model	2
2 Extreme events in the generic Lotka Volterra system	11
3 How extreme are the extreme events?	23
3.1 A measure for the extremeness of events	23
3.2 Results of simulation	24
3.3 What is happening for small values of C ?	27
4 Window of quenched activity	31
4.1 Bifurcation diagrams	31
4.2 Bifurcation diagrams for our system	33
4.3 Mass-extinctions brought about by coupling	35
Bibliography	41

List of Figures

1.1	Schematic of the ring of coupled patches. Image taken from Chaurasia et al. [CVS20]	3
1.2	Variation of u , v and w in a single patch without coupling. The dotted black line represents the mean value of the variable in each case. The solid black line represents, in each case, the value of the variable which is ten times the standard deviation away from the mean.	4
1.3	Instability in an uncoupled patch with very high value of w in initial conditions. The dotted and the solid black lines have the same meaning as in Figure 1.2.	5
1.4	Variation of u , v and w in a representative patch with coupling according to equations 1.2, with $C = 1$. The dotted black line represents the mean value of each variable. The solid black line represents the value which is ten times the standard deviation away from the mean.	6
1.5	Variation of u , v and w in a representative patch without coupling according to equations 1.1 for a much longer time scale than Figure 1.2 The dotted black line represents the mean value of each variable. The solid black line represents the value which is ten times the standard deviation away from the mean.	8
1.6	Variation of u_{max} , v_{max} and w_{max} , the global maximum of the vegetation population, prey population and the predator population respectively in a patch with $N = 100$ on an interval of time $T = 50$ with increasing coupling constant C . The values plotted here are scaled by dividing the corresponding values at $C = 0.0$. Image taken from [CVS20]	9
1.7	Variation of u_{max} , v_{max} and w_{max} , the global maxima of the vegetation population, prey population and the predator population respectively in a patch with $N = 100$ with increasing coupling constant C , averaged over 50 initial conditions. The values plotted here are scaled by dividing the corresponding values at $C = 0.0$	10
2.1	Phase space trajectories of 5 different iterations of the two-level Lotka Volterra system described by equations 2.1.	12
2.2	v and w as a function of time for the system defined by equations 2.1	13
2.3	v and w as a function of time for the system defined by equations 2.2 for one representative patch.	14

2.4	Phase space for one patch when extreme events occur in the two-level system.	15
2.5	Population levels of prey v a function of both time and space for the system defined by equations 2.2, for a system of 100 patches, and $C = 1$. Most of the plot is black or blue, which means the population remains low at most patches for most times. However, there are sparsely scattered reddish-yellow spots, representing extreme events. These spots are really thin, as the high levels of population are sustained only momentarily. These are not scattered according to any pattern. The extreme events appear to be less frequent than those in predator populations. See Figure 2.6.	16
2.6	Population levels of predator w a function of both time and space for the system defined by equations 2.2, for a system of 100 patches, and $C = 1$. Most of the plot is black or blue, which means the population remains low at most patches for most times. However, there are sparsely scattered reddish-yellow spots, representing extreme events. These spots are really thin, as the high levels of population are sustained only momentarily. These are not scattered according to any pattern. The extreme events appear to be more frequent than those in prey populations. See Figure 2.5.	18
2.7	Frequency of extreme events in prey as function of C	19
2.8	Frequency of extreme event in predator as function of C	20
2.9	Ratio of frequency of extreme events in prey to that in predator as a function of C	20
2.10	Probability distribution of the time intervals between two successive extreme events in the prey population- histogram from the raw data and the exponential best fit.	21
2.11	Probability distribution of the time intervals between two successive extreme events in the predator population- histogram from the raw data and the exponential best fit.	22
3.1	The dependence of $\langle v_{max} \rangle$ on the coupling constant C for discrete values between 0 and 3, separated by 0.2. The points have been joined. The solid line joins the points obtained when the averaging was performed over 50 initial conditions, and hence is the most reliable. The dashed line joins points that were obtained upon averaging over 20 initial conditions, and the dotted line joins the points that were obtained over 5 initial conditions.	25

3.2	The dependence of $\langle v_{max} \rangle$ on the coupling constant C for discrete values between 0 and 3, separated by 0.2. The points have been joined. The solid line joins the points obtained when the averaging was performed over 50 initial conditions, and hence is the most reliable. The dashed line joins points that were obtained upon averaging over 20 initial conditions, and the dotted line joins the points that were obtained over 5 initial conditions.	26
3.3	The dependence of $\langle v_{max} \rangle$ on the coupling constant C for discrete values between 0 and 1, separated by 0.04, averaged over 100 randomized initial conditions. The points have been joined by a line.	28
3.4	The dependence of $\langle w_{max} \rangle$ on the coupling constant C for discrete values between 0 and 1, separated by 0.04, averaged over 100 randomized initial conditions. The points have been joined by a line.	29
4.1	Bifurcation diagram for the logistic map.	32
4.2	Bifurcation diagram comprising of all the local maximas as coupling is varied, for prey.	34
4.3	Bifurcation diagram comprising of all the local maximas as coupling is varied, for predator.	35
4.4	Bifurcation diagram comprising of all the local maximas as coupling is varied, for prey.	36
4.5	Bifurcation diagram comprising of all the local maximas as coupling is varied, for predator.	37
4.6	Time-series for a representative patch at $C \sim 0.44$. Note that the prey gets extinct fairly quickly and the predator population sees a continuous series of spurts. However, these spurts are relatively smaller and none of these are extreme events according to our definition.	38
4.7	Time-series for a representative patch at $C \sim 0.44$. Note that the predator gets extinct fairly quickly and the prey population sees a continuous series of spurts. However, these spurts are relatively smaller and none of these are extreme events according to our definition.	38
4.8	The extinction of either of the species on the 100 patches- at a representative instant of time after transience. Blue patches represent patches which have only the predator present, which means, the prey has gone extinct. Green patches represent those where only the prey survives, and hence the predator has gone extinct. Aqua circles represent the patches on which neither has gone extinct.	39

*Dedicated to all the frontline health workers across
the globe, who are bravely fighting this crisis of the
Covid-19 pandemic at the forefront.*

Chapter 1

Advent of extreme events in Lotka Volterra systems

1.1 Introduction

Extreme events have generated quite a lot of interest, due to their very broad spectrum of relevance [[AJK06](#)]. They are prevalent in power grids, economic shocks, weather catastrophes etc. An extreme event is said to have occurred if a dynamical variable changing as a function of time suddenly takes a value which is several standard deviations away from its time-average. It should be noted that for extreme events to occur, the dynamical variable should not only suddenly shoot up or dip down, but should also return to the ‘usual’ values immediately. For if it does not return and stays at those high or low values for considerable time, the time-average of the system is also pushed up or down. Thereby, the event may not be said to be ‘extreme’. Hence, sudden instabilities in system, which lead to a sudden explosion or decimation in the values of a dynamical variable are not typically instances of extreme events.

Generic mechanisms of occurrence of extreme events in deterministic systems are not well-understood. Most of the models which are known to generate extreme events have an element of stochasticity, intrinsic randomness in their nature.

1.2 Emergence of extreme events in an ecological model

In this section, we describe a mechanism to generate extreme events in a deterministic system, unearthed by Chaurasia et al. [CVS20] that forms the basis of the work that forms this thesis.

Consider a system of three species of organisms coupled through Lotka Volterra type of interactions. Let $u(t)$, $v(t)$ and $w(t)$ be the variables representing the population of some vegetation, prey and predator respectively. Let the dynamics of these variables be governed according to the following equations.

$$\begin{aligned}\dot{u} &= au - \alpha_1 f_1(u, v) \\ \dot{v} &= -bv + \alpha_1 f_1(u, v) - \alpha_2 f_2(v, w) \\ \dot{w} &= -c(w - w^*) + \alpha_2 f_2(v, w)\end{aligned}\tag{1.1}$$

We need to know the explicit functional forms of f_1 and f_2 . The functional form of $f_1(u, v)$ is given by $f_1(u, v) = \frac{uv}{1+ku}$. The function $f_2(v, w)$ is defined as $f_2(v, w) = vw$, and is thus, the usual Lotka-Volterra term between the prey v and the predator w .

This system, with the choice of parameters $a = 1.0$, $b = 1.0$, $c = 10.0$, $w^* = 0.006$, $\alpha_1 = 0.5$, $\alpha_2 = 1.0$, $k = 0.05$ explains the population-dynamics of the snowshoe hare and the Canadian lynx [BHS99].

Now consider a larger system of these three species. Let there be several (of the order of 100) patches in this system, each of which consists of the system of three species as described above. Let these patches be arranged on a ring, such that each of the patches is coupled only to the two nearest neighbors, one on either side (see Figure 1.1). The coupling is such that the predator of each patch can predate on the prey of the two coupled patches.

More specifically, if u_i , v_i and w_i refer to the populations of vegetation, prey and predator respectively on the i^{th} patch, the dynamical equations governing these variables are given by

$$\begin{aligned}\dot{u}_i &= au_i - \alpha_1 f_1(u_i, v_i) \\ \dot{v}_i &= -bv_i + \alpha_1 f_1(u_i, v_i) - \alpha_2 f_2(v_i, w_i) - \frac{C}{2} \{v_i w_{i-1} + v_i w_{i+1}\} \\ \dot{w}_i &= -c(w_i - w^*) + \alpha_2 f_2(v_i, w_i) + \frac{C}{2} \{w_i v_{i-1} + w_i v_{i+1}\}\end{aligned}\tag{1.2}$$

Equations 1.2 are different from equations 1.1 only in the presence of the terms shown in red. The constant C defines the strength with which the neighboring patches are coupled.

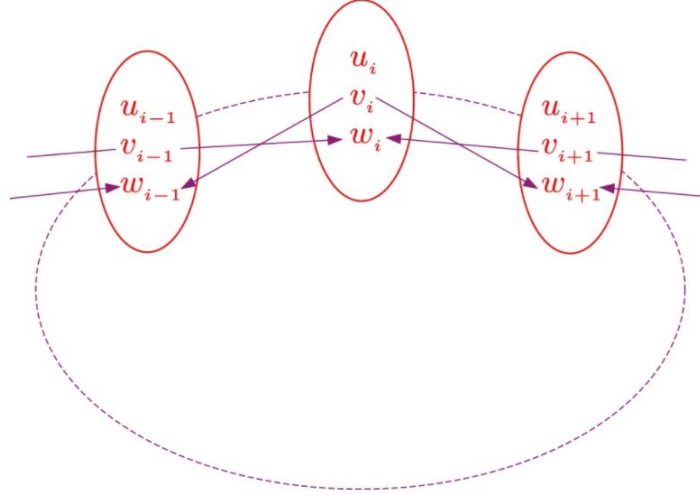


FIGURE 1.1: Schematic of the ring of coupled patches. Image taken from Chaurasia et al. [CVS20]

We integrate the system 1.1 with initial u , v and w to be of the order of 0.1. The results are shown in Figure 1.2.

It is evident that after an initial transience, the system exhibits periodic dynamics. It should be noted that the abrupt high spurts in these time-series' are not extreme events, as these are periodic, whereas consecutive extreme events, by definition, should be uncorrelated in time. This observation is in agreement with the results of Charuasia et al. [CVS20].

If this same system is evolved with initial conditions such that the initial value of w is of the order of 100, the system is no more periodic, but is unstable. Thus, there are limits to the robustness of this model system (Figure 1.3).

How do the dynamics look for the system when it is coupled as described by equations 1.2? The time-series for a representative patch in a ring of 100 such patches is shown in the Figure 1.4. The value of the coupling constant C in our computations was $C = 1$.

It turns out that in predator populations, there are sudden spurts of growth, that are at least ten standard deviations away from the mean. These events occur irregularly in time. They are also uncorrelated in space and time. These are extreme events.

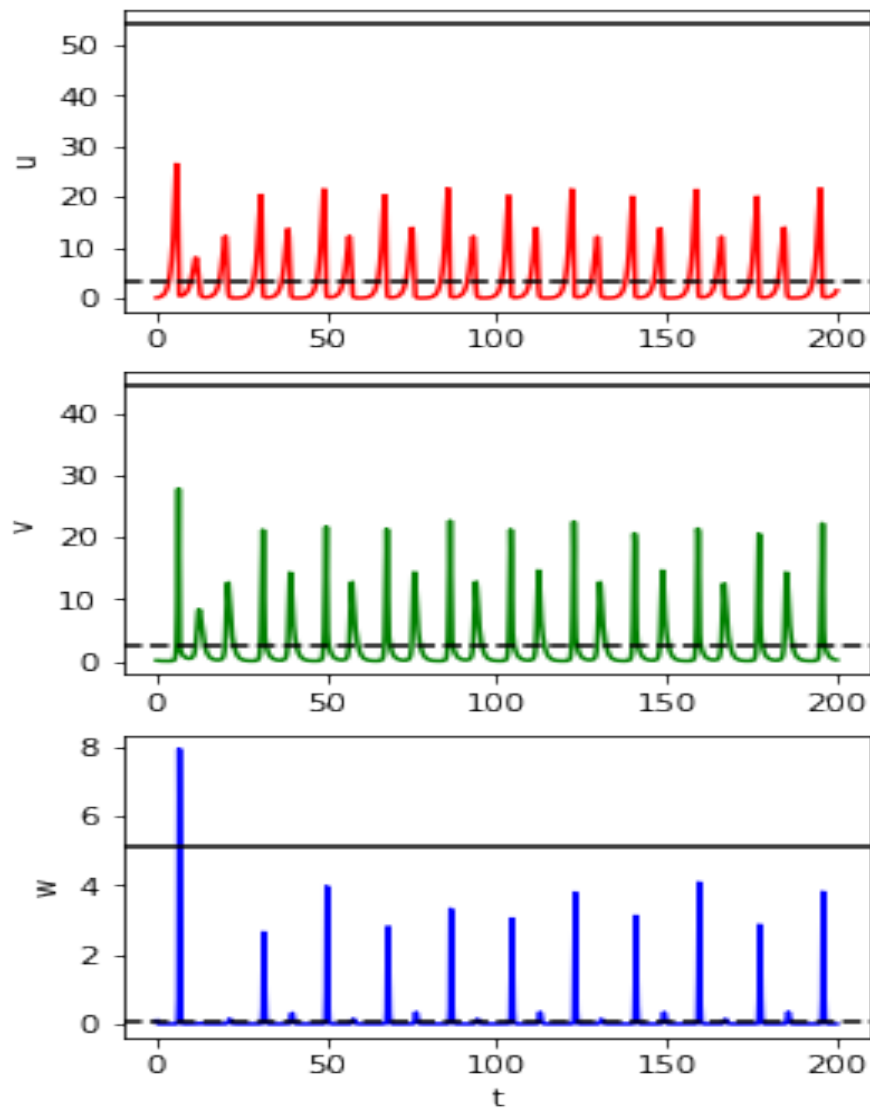


FIGURE 1.2: Variation of u , v and w in a single patch without coupling. The dotted black line represents the mean value of the variable in each case. The solid black line represents, in each case, the value of the variable which is ten times the standard deviation away from the mean.

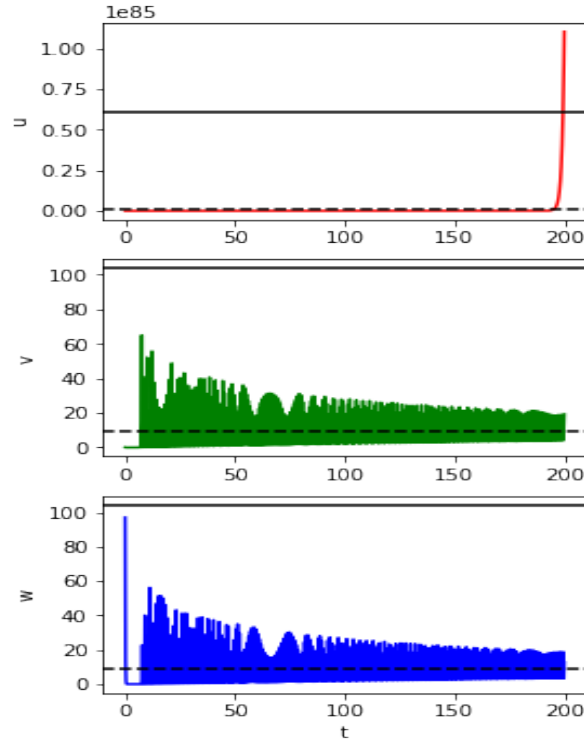


FIGURE 1.3: Instability in an uncoupled patch with very high value of w in initial conditions. The dotted and the solid black lines have the same meaning as in Figure 1.2.

This observation is also in agreement with the results of Chaurasia et al. [CVS20]. Chaurasia et al. do not note the existence of the instability of the system as described in Figure 1.3. All other observations described above are in agreement with their results, and have been reproduced and verified independently by the author for several different iterations, and with varying values of the relevant parameters. It has also been independently confirmed that these events are uncorrelated in space and time, as noted by them.

It must also be noted that the kind of instability seen in Figure 1.3 is also obtained even when the initial values for all the u_i 's, v_i 's and the w_i 's are chosen to be small, but the coupling constant C in the equations 1.2 above is made large- of the order of 100.

It must also be noted that on the long time-scale, the time-series of u , v and w in Figure 1.2 is not as simple as it appears to be. If the time series is plotted for a longer time scale, one can see that there is more to it. The height of the periodic maximas does not remain constant, and it varies with time exhibiting interesting patterns. The time series over a longer scale is shown in Figure 1.5.

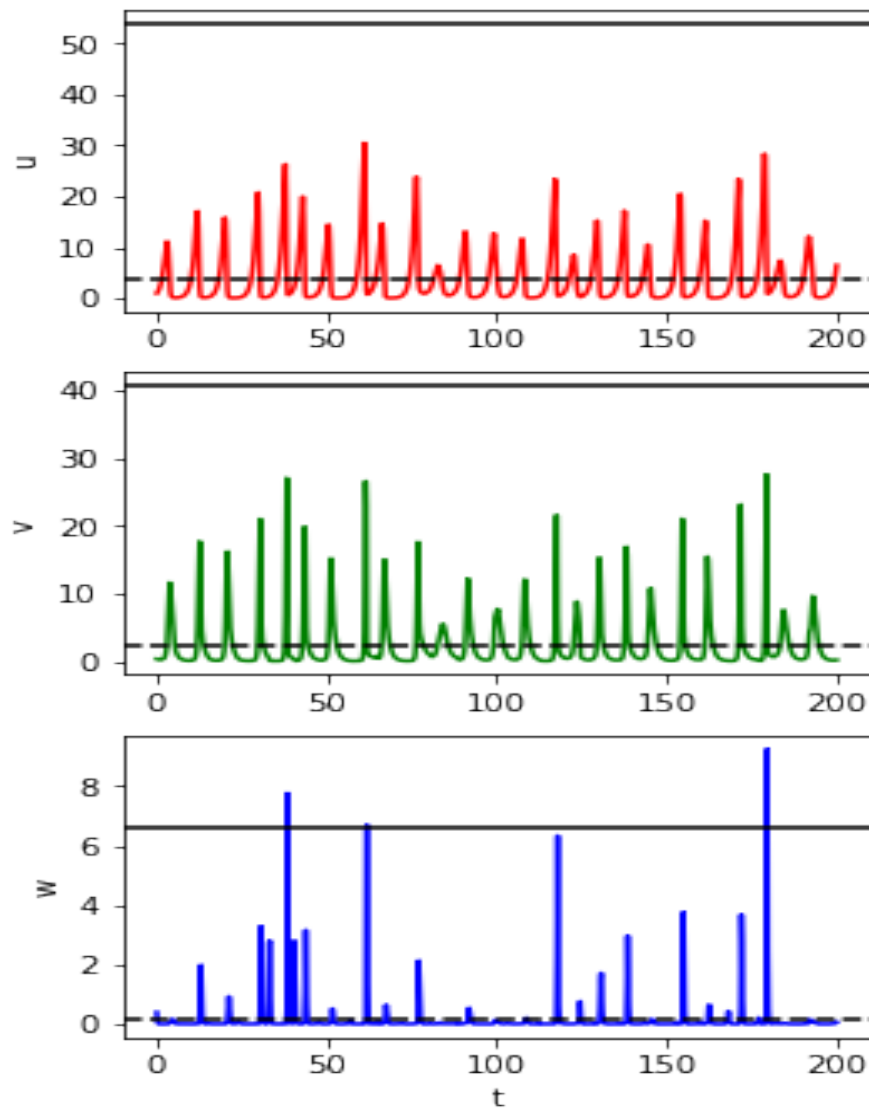


FIGURE 1.4: Variation of u , v and w in a representative patch with coupling according to equations 1.2, with $C = 1$. The dotted black line represents the mean value of each variable. The solid black line represents the value which is ten times the standard deviation away from the mean.

For the coupled system (1.2), it was also found that the system is not always stable. Even when the initial conditions are taken to be small (smaller than 1.0 for all the three variables), the system can encounter a blow-up, which means that one of the variables increases without bounds.

It should be borne in mind that the initial values of u_i , v_i and w_i should be chosen randomly independently for different patches. In my observation, it does not matter what underlying probability distribution is used to generate the initial values of these dynamical variables. Extreme events do occur as long as the values of initial conditions are uncorrelated, and are not too large.

It is worth emphasizing that the occurrence of extreme events in this system is without any external introduction of noise or stochasticity. It is just the different unsynchronized values of the populations of vegetation, prey and predator that give rise to them.

Chaurasia et al. [CVS20] also show how the global maximum of the vegetation population u_{max} , the prey population v_{max} and the predator population w_{max} for $N = 100$ in a ring change as the coupling constant C is increased from 0 to 1. They find that each of these three quantities increase monotonically as a function of C , at least in the range of C from 0 to 1. The dependence of w_{max} on C changes dramatically at around $C \sim 0.25$. This figure from their paper is reproduced as Figure 1.6.

We tried to reproduce the Figure 1.6 in our work. We integrated the system for 200 time units for a given value of C , and looked for the global maximum among all the local maxima on all the patches. We repeat this procedure several times for the same value of C , each time choosing a randomly chosen set of initial conditions and noting the global maximum in the end. We finally take the average of all the global maxima we collected. Then we increased the C a little, and again found the average global maximum with integration for 200 time units each time. Note that this is a computationally expensive procedure. It becomes more and more computationally expensive as the sample size for random initial conditions over which the global maximum is found for a fixed value of C is increased. The expensiveness is compounded by the fact that in rare cases, one of the variables might just blow up. As the sampling over initial conditions is increased, the system probability of blow-ups increases. (We also noted that the probability of blow-up also increased with increasing C .) It should also be noted that in the ring of 100 patches, even if one of the patches blows up, the whole integration has to be done again with a different set of initial conditions.

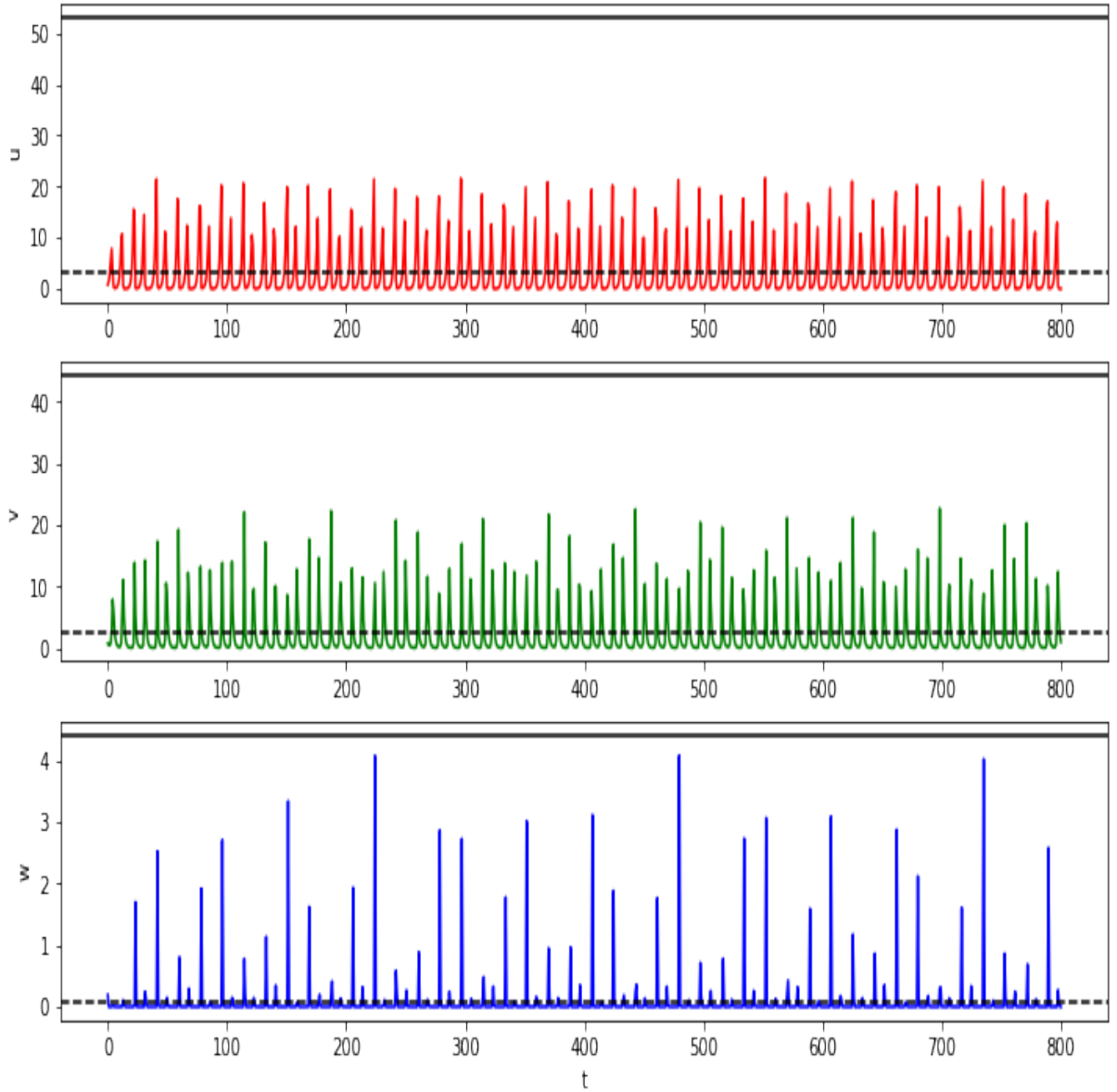


FIGURE 1.5: Variation of u , v and w in a representative patch without coupling according to equations 1.1 for a much longer time scale than Figure 1.2 The dotted black line represents the mean value of each variable. The solid black line represents the value which is ten times the standard deviation away from the mean.

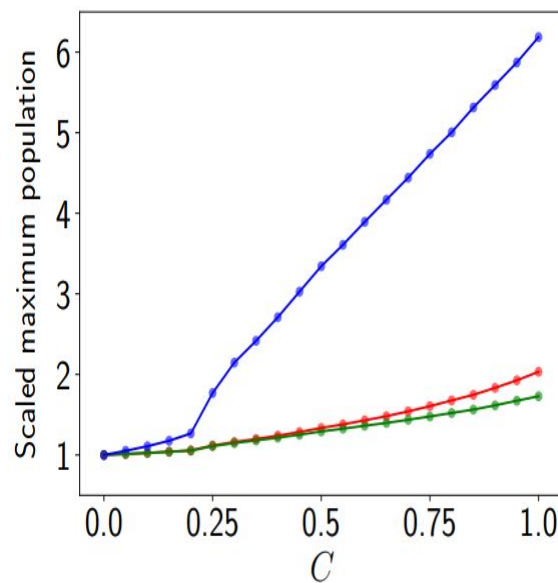


FIGURE 1.6: Variation of u_{max} , v_{max} and w_{max} , the global maximum of the vegetation population, prey population and the predator population respectively in a patch with $N = 100$ on an interval of time $T = 50$ with increasing coupling constant C . The values plotted here are scaled by dividing the corresponding values at $C = 0.0$. Image taken from [CVS20]

We found that if we calculate the global maximum for a given value of C for small sample sizes of initial conditions (~ 10), our figures did not resemble the trends in Figure 1.6. But we did find that as the sample of initial conditions over which the values are averaged over is made larger, the figures start to resemble Figure 1.6 more and more.

We show the figure that we got by averaging over 50 initial conditions- Figure 1.7. Note that the blue curve is slightly separated from the red and the green curves, which plot the corresponding quantity for the prey and vegetation. We found that the blue curve separates more and more as the number of initial conditions is increased. This can be explained by observing that very strong extreme events are rare in occurrence. If we sample for more and more time, the probability of occurrence of those rare strong extreme events becomes more and more substantial. But since we consider only the single global maximum in the whole ring, these rare but significantly strong events have a significant effect on the curve. We expect that as we average for really long times, we shall reproduce Figure 1.6 exactly. This feature of the averaged global maximum depending upon the size of sampling of events will re-surface again in Chapter 3.

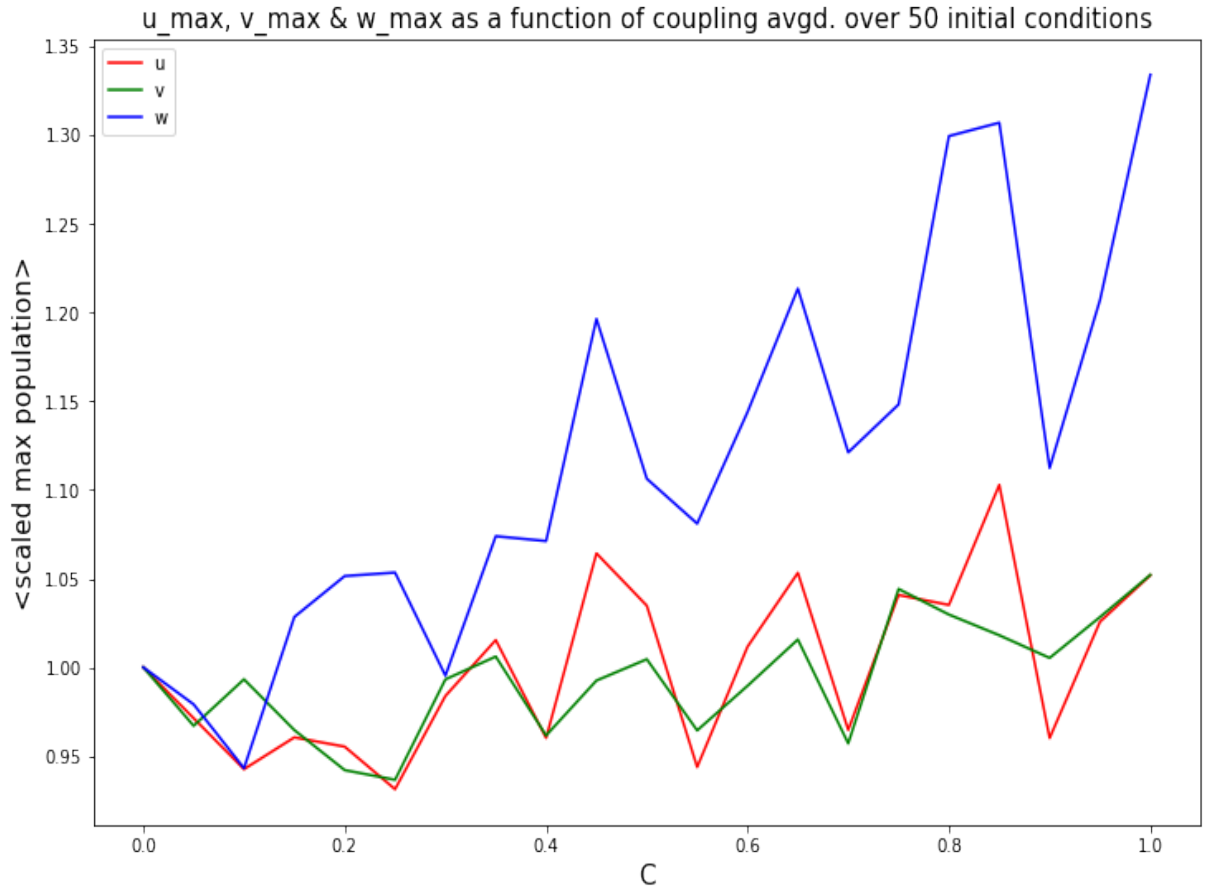


FIGURE 1.7: Variation of u_{max} , v_{max} and w_{max} , the global maxima of the vegetation population, prey population and the predator population respectively in a patch with $N = 100$ with increasing coupling constant C , averaged over 50 initial conditions. The values plotted here are scaled by dividing the corresponding values at $C = 0.0$.

Chapter 2

Extreme events in the generic Lotka Volterra system

In light of the emergence of extreme events in the system described above without any noise or stochasticity, several questions arise. One of the fundamental questions is whether the emergence of extreme events in this system is something special, in the sense of this being specific to this very system, or is it a more generic feature of such systems? Also, why do the extreme events occur only in the predator populations? Is there a deeper way to see this?

To shed some light on the answers to these questions, we look at a model that the author studied using numerical computations. Consider the Lotka Volterra system between **two** species (unlike three- which was the case in Chapter 1), described by the following dynamical equations.

$$\begin{aligned}\dot{v} &= \alpha v - \beta vw \\ \dot{w} &= -\gamma w + \delta vw\end{aligned}\tag{2.1}$$

where α , β , γ and δ are all positive constants.

These equations describe a prey and predator interacting through the Lotka Volterra interactions. The variable v represents the prey and w represents the predator. The reader should distinguish between the use of α here and α_1 and α_2 in equations 1.1 and 1.2 respectively.

We choose to work with $\alpha = 0.1$, $\beta = 0.5$, $\gamma = 0.3$ and $\delta = 0.4$.

Let us put to rest a very important question before proceeding further. Do the values of α , β , γ and δ specified above have anything special in them. The answer appears to be yes, but not a very resounding one. The conclusions that we draw with these values (to be described in detail later) are NOT

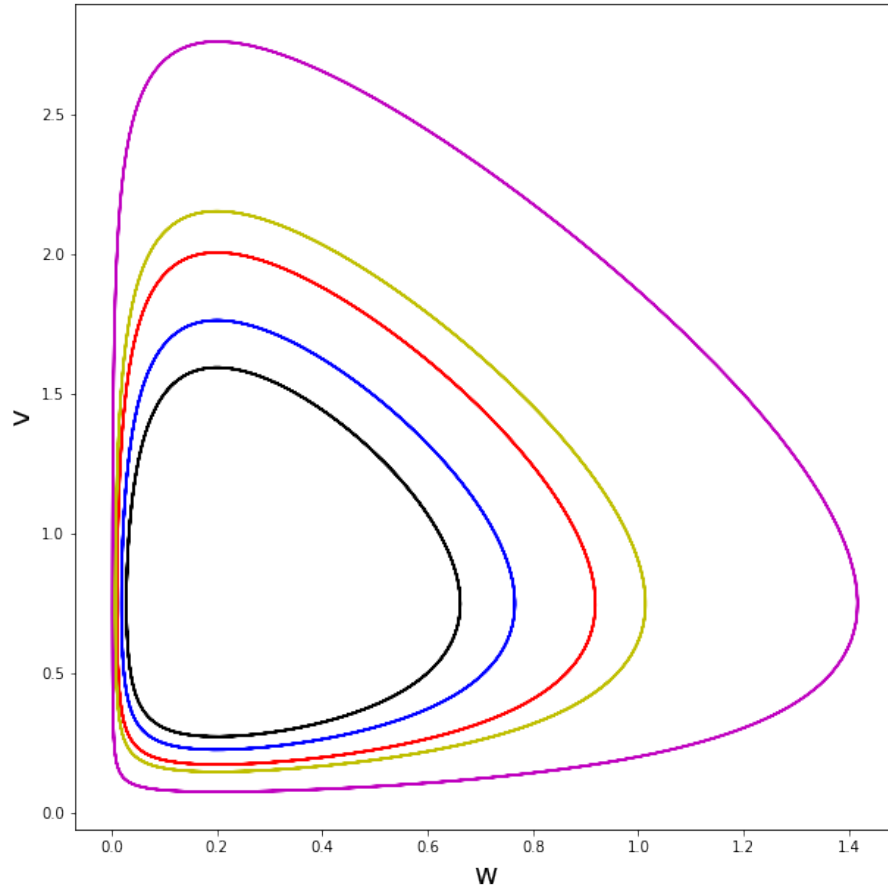


FIGURE 2.1: Phase space trajectories of 5 different iterations of the two-level Lotka Volterra system described by equations 2.1.

extendable to all two-level simple Lotka Volterra systems. In fact, we could not get the kinds of interesting effects we get with these values in any other system. However, some other systems behave somewhat similarly. Moreover, we are going to see later that the relevant behaviour of the system is very very heavily dependent upon the strength of a coupling we are going to introduce below. It is very similar to the coupling used in Chapter 1. There could be some special values of the strengths of coupling that could lead to the same effects in some other Lotka Volterra systems. The question is an open one, but is not trivial. The reader should keep this in mind. Now let us return to studying our system.

To understand this system better, we can plot the phase space trajectories of the system. I randomly generated initial conditions between 0 and 1 for both v and w , and generated the resulting phase space. I repeated this procedure a total of five times, and plotted the thus generated 5 phase space trajectories simultaneously. The plot is shown in Figure 2.1.

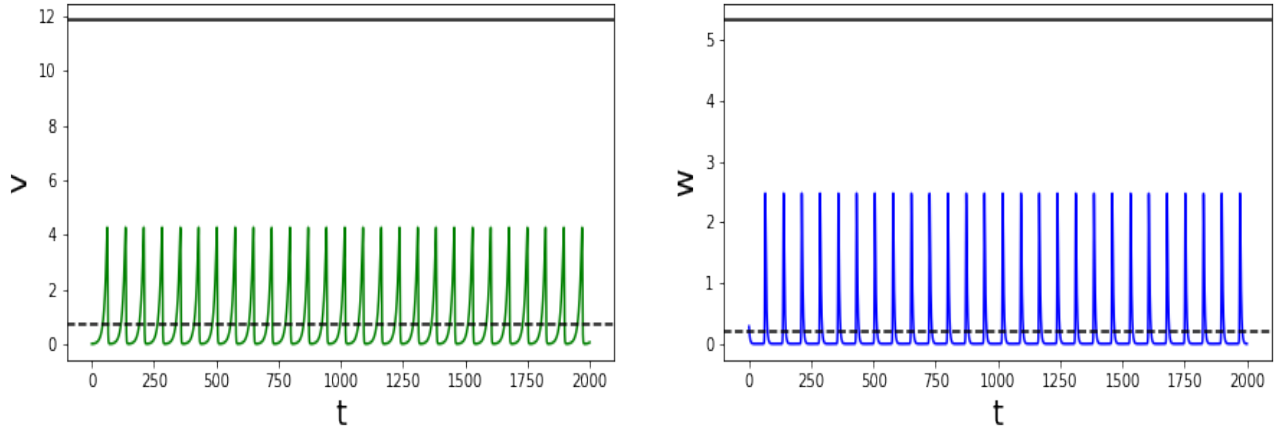


FIGURE 2.2: v and w as a function of time for the system defined by equations 2.1

The time-series for v and w are shown in Figure 2.2.

As can be seen from both Figure 2.1 and Figure 2.2, the system is periodic in both the dynamical variables.

Now consider patches of such prey-predator systems arranged in a ring, and we couple the patches in the same way as we did for the three species system in Chapter 1, that is, the predators of each patch are made to predate on the prey of neighboring two patches. The dynamical equations would then take the form:

$$\begin{aligned}\dot{v}_i &= \alpha v_i - \beta v_i w_i - \frac{C}{2} \{v_i w_{i-1} + v_i w_{i+1}\} \\ \dot{w}_i &= -\gamma w_i + \delta v_i w_i + \frac{C}{2} \{w_i v_{i-1} + w_i v_{i+1}\}\end{aligned}\tag{2.2}$$

As before, the terms in red arise due to coupling of the neighbouring patches, and C refers to the strength of coupling.

The time-series for a representative patch in a ring of 100 such patches, for $C = 3.0$ is shown for both the variables in Figure 2.3.

In Figure 2.3, the black dotted lines represent the mean value of the two dynamical variables, while the black solid lines represent the value of the variables ten standard deviations away from the mean, as in Figures 1.2, 1.3 and 1.4. It is evident that both v and w at times, suddenly attain values which are more than ten standard deviations away from the mean. Hence, it appears that these are extreme events. If these are extreme events indeed, we have a system that has extreme events in both the prey and the predator populations, unlike the system studied before. Before concluding that these sudden spurts are actually extreme events, one should confirm that these occur in an

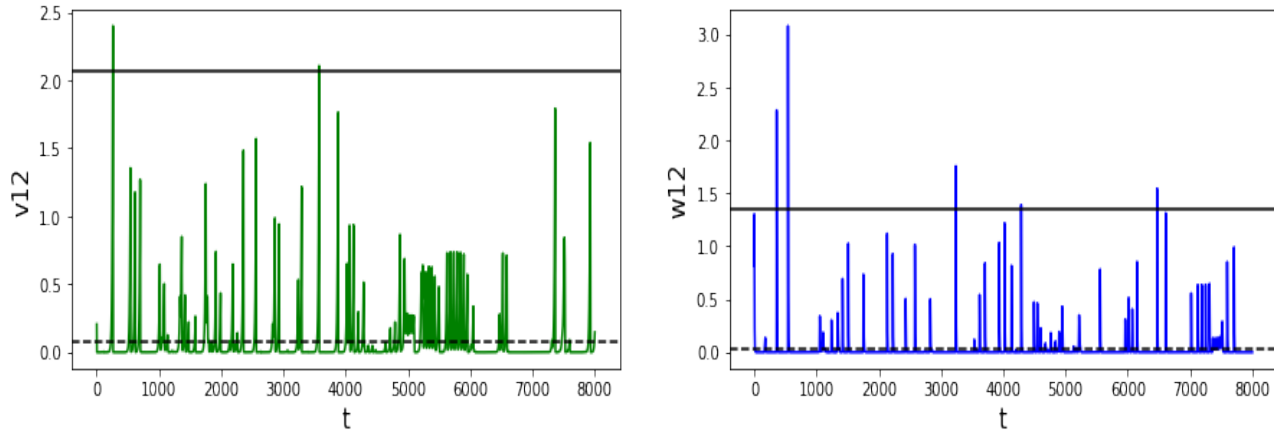


FIGURE 2.3: v and w as a function of time for the system defined by equations 2.2 for one representative patch.

uncorrelated fashion in both space and time. We shall address this question later, and we will find that these are actually extreme events. But perhaps it is important to pause and ponder over this result. It appears that the emergence of extreme events in the system described by Chaurasia et al. [CVS20] is not a special case, but it is a general feature of such coupled Lotka Volterra systems. Moreover, in that study, the extreme events were prevalent only in the predator populations, whereas in this system, they are prevalent in both the prey and predator populations. It appears that something in that system was ‘suppressing’ them in the prey populations. It could be the functional forms of the differential equations, or it could be the presence of the additional trophic level of vegetation.

It is instructive to look at the phase space of one v and one w —both taken from the same patch, and see how both these variables change. We show this in the Figure 2.4. The figure shows v and w from one patch described by the equations 2.2 with $C = 3.0$, after removing some initial transience. The phase space excursion shows that it never happens that both v and w increase together. If this were happening, the part of the phase space in the top-right would also have been visited by the trajectory. However, we see that it is either the v that takes values much larger than the usual values, or w that does so, but never both. This conclusion has been verified by plotting the phase space multiple times.

Figure 2.5 shows the spatiotemporal variation of the variable v representing the prey population as function of time on all the 100 different patches.

Phase space of the variables representing prey and predator populations on one patch with extreme events

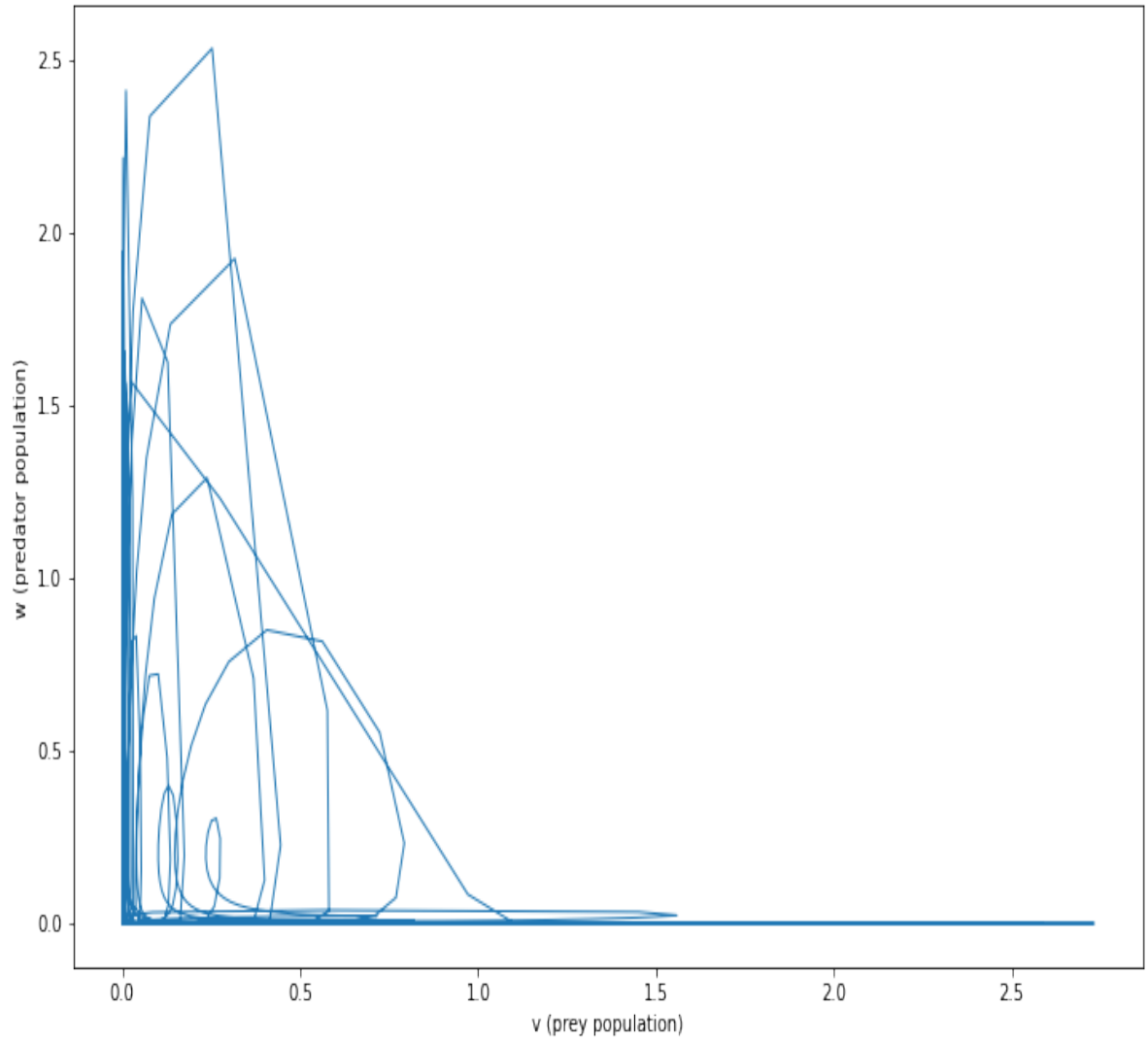


FIGURE 2.4: Phase space for one patch when extreme events occur in the two-level system.

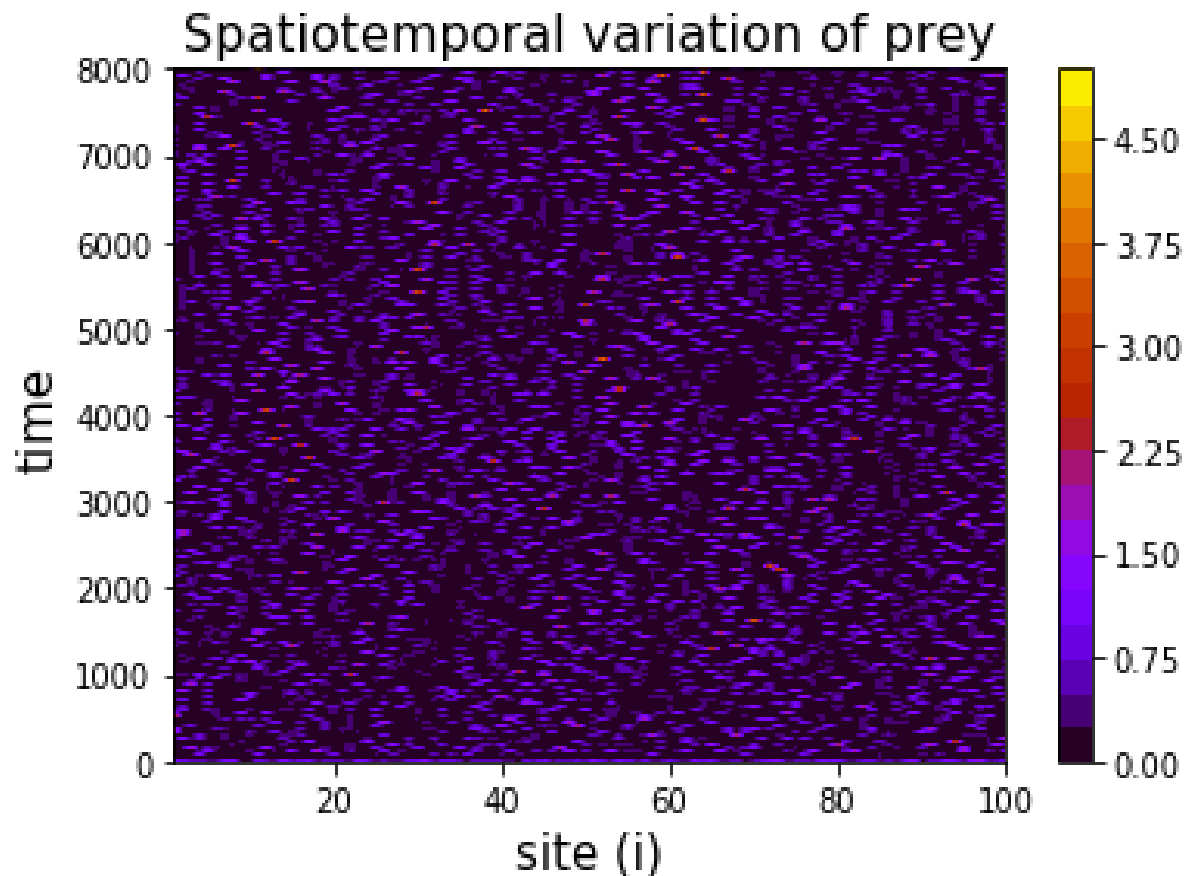


FIGURE 2.5: Population levels of prey v a function of both time and space for the system defined by equations 2.2, for a system of 100 patches, and $C = 1$. Most of the plot is black or blue, which means the population remains low at most patches for most times. However, there are sparsely scattered reddish-yellow spots, representing extreme events. These spots are really thin, as the high levels of population are sustained only momentarily. These are not scattered according to any pattern. The extreme events appear to be less frequent than those in predator populations. See Figure 2.6.

Similarly, Figure 2.6 shows the spatiotemporal variation of the variable w representing the predator-population as a function of time on different patches.

Figures 2.5 and 2.6 show the populations of the prey and predator respectively, simultaneously in space and time. High population events are represented on these plots by reddish or yellow fine spots. It can be inferred from these that these high population events are uncorrelated in both space and time, and hence can be classified as being extreme events.

From these (Figures 2.5 and 2.6) plots, it seems that the frequency of extreme events in the case of predators is higher than that of prey. Moreover, the occurrence of extreme events has gone from being non-existent at $C = 0$ to being fairly common at $C = 3.0$. How does the frequency of extreme events increase as C is varied, for both prey and predator? To answer these questions, a good amount of statistics need to be collected. To do so, same system of 100 patches in a ring was integrated with some chosen value of C for 2000 units of time, and the number of extreme events occurring in each patch in prey as well as predator populations were counted. In this counting, without loss of any generality, just for the sake of ease of collecting statistics, any event that was 5 standard deviations away from the mean was called an extreme event. We do not expect the properties of these events to change just with our changing definition. An event 5 standard deviations away if also fairly away from the mean and can be called 'extreme'. This whole procedure was repeated 5 times, each time initializing the system with randomly chosen initial values of v_i and w_i for all i running from 1 to 100, and the extreme events in all the patches for both the variables were counted as before. This whole procedure was repeated for the values of C ranging from 0 to 3.5 in steps of 0.1. Finally, the number of extreme events counted were divided by $5 \times 2000 = 10,000$ to calculate the frequency of extreme events, for each value of C . (5 because the process was repeated for five times for each value of C and 2000 because this was the time for which the system was integrated in each iteration.) Figures 2.7, 2.8 and 2.9 summarize the results.

The first plot (Figure 2.7) shows the variation of the frequency of extreme events in the prey population as a function of C , the second plot (Figure 2.8) shows the same in the predator population, while the third plot shows the variation of the ratio of the frequencies of extreme events in prey to those in predator. It can be seen that the frequency of extreme events increases both in prey and predator as the coupling between the patches increases. However, it is clear that the number of extreme events saturates as C increases, and

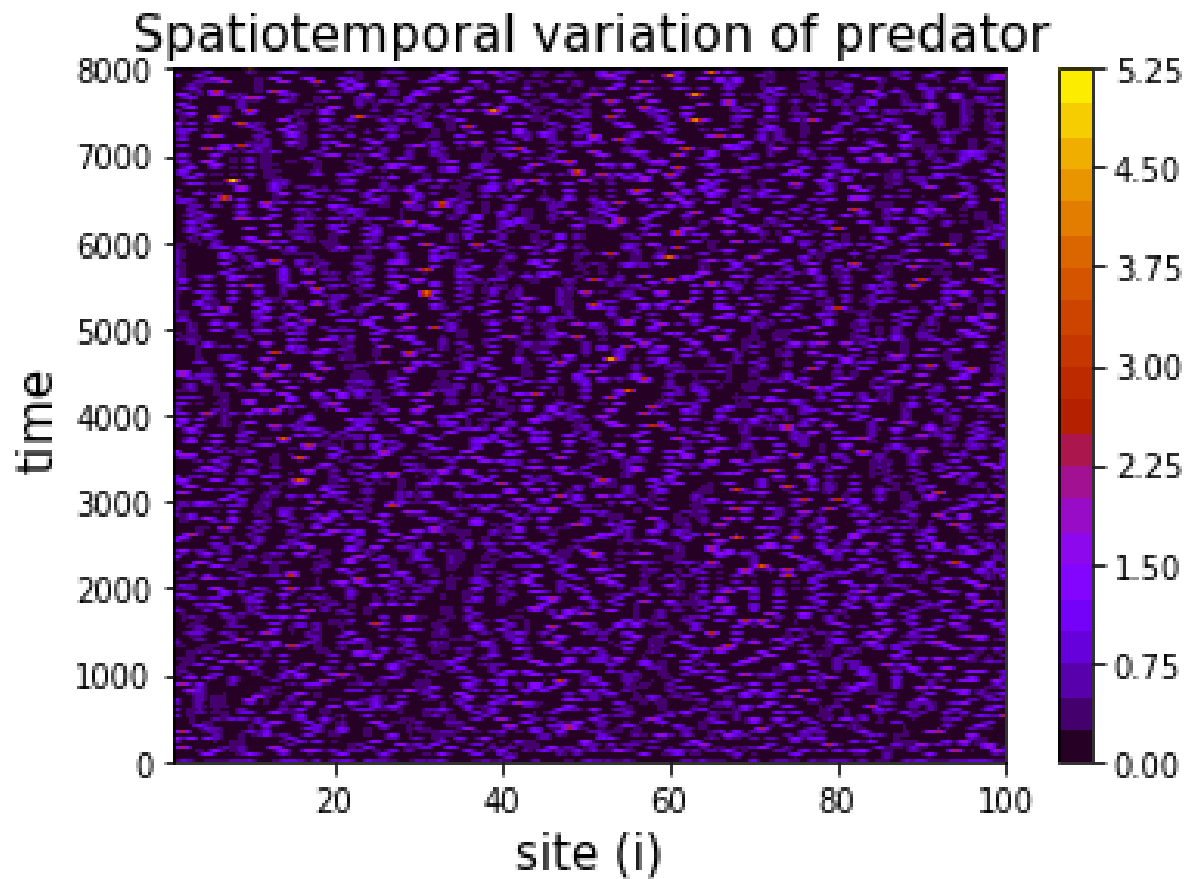


FIGURE 2.6: Population levels of predator w a function of both time and space for the system defined by equations 2.2, for a system of 100 patches, and $C = 1$. Most of the plot is black or blue, which means the population remains low at most patches for most times. However, there are sparsely scattered reddish-yellow spots, representing extreme events. These spots are really thin, as the high levels of population are sustained only momentarily. These are not scattered according to any pattern. The extreme events appear to be more frequent than those in prey populations. See Figure 2.5.

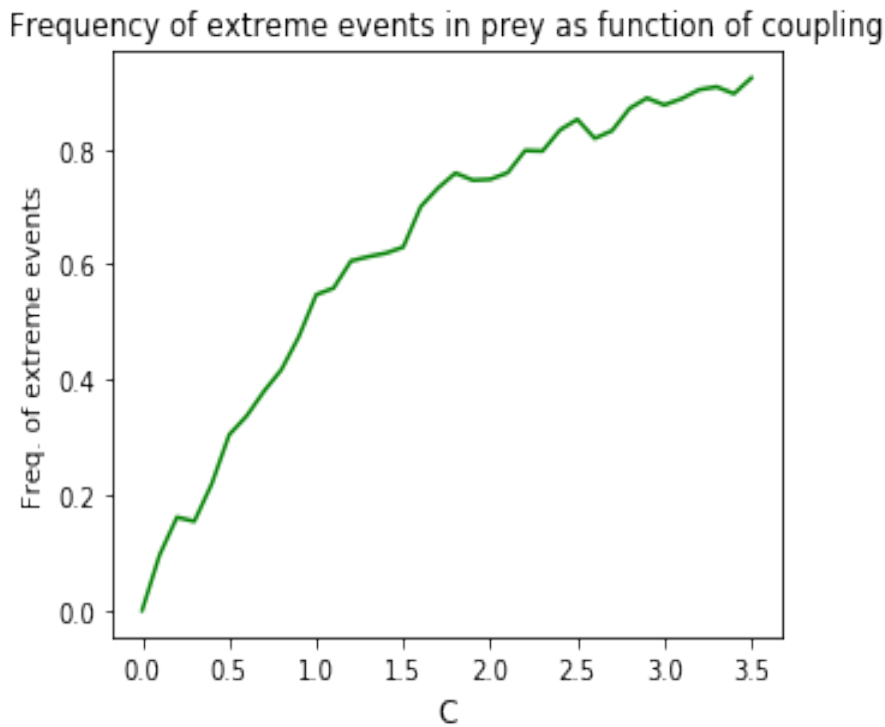
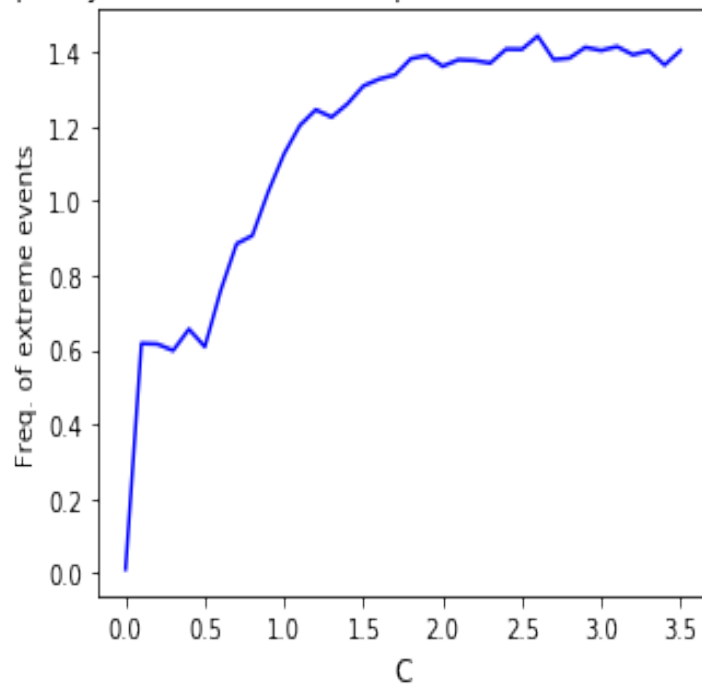


FIGURE 2.7: Frequency of extreme events in prey as function of C .

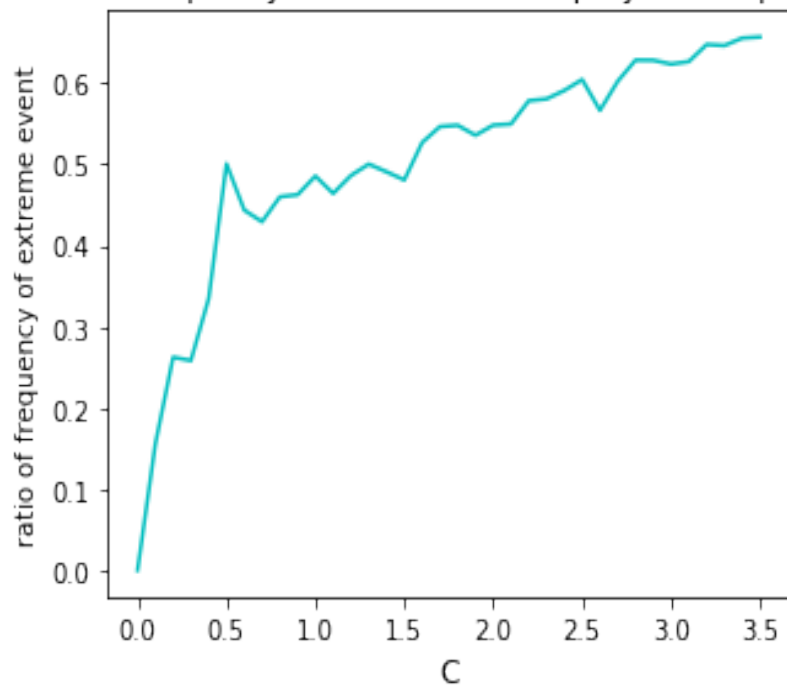
it saturates rather more rapidly in case of predators. The third plot clearly shows that the frequency of extreme events is less in prey than predator, as the ratio of the former to the latter remains below 1. However, this ratio increases as a function of C , showing that the gap decreases as C is increased.

We can also see in another way that these events are uncorrelated. Let's look at the distribution of the time interval between two successive extreme events on all the patches. Events that occur in time in an uncorrelated fashion, but have a constant average rate of occurrence are expected to follow a Poisson distribution. The time-difference between two successive such events is expected to follow an exponential probability distribution (also known as the 'waiting time distribution'). In Figure 2.10 we plot the time difference between two successive extreme events in the prey populations from a large data set. We integrate the whole system for 8000 time units a total of 25 times, and make a list of the time differences between two successive extreme events. We plot a histogram of the data, and also show the best-fit exponential distribution. It is evident that the data indeed follows an exponential distribution. Figure 2.11 shows the corresponding plot for the predator distribution, which is also seen to follow an exponential distribution.

Frequency of extreme events in predator as a function of coupling

FIGURE 2.8: Frequency of extreme event in predator as function of C .

Ratio of frequency extreme events in prey to that predator

FIGURE 2.9: Ratio of frequency of extreme events in prey to that in predator as a function of C .

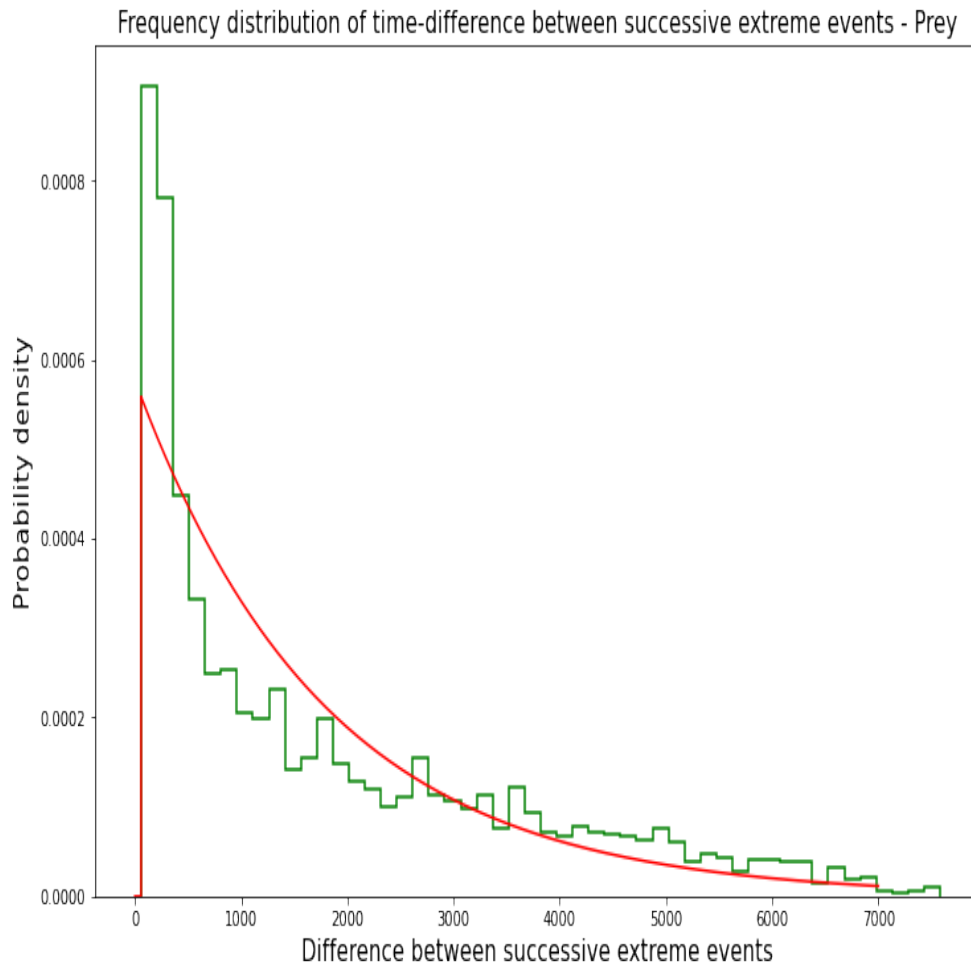


FIGURE 2.10: Probability distribution of the time intervals between two successive extreme events in the prey population-histogram from the raw data and the exponential best fit.

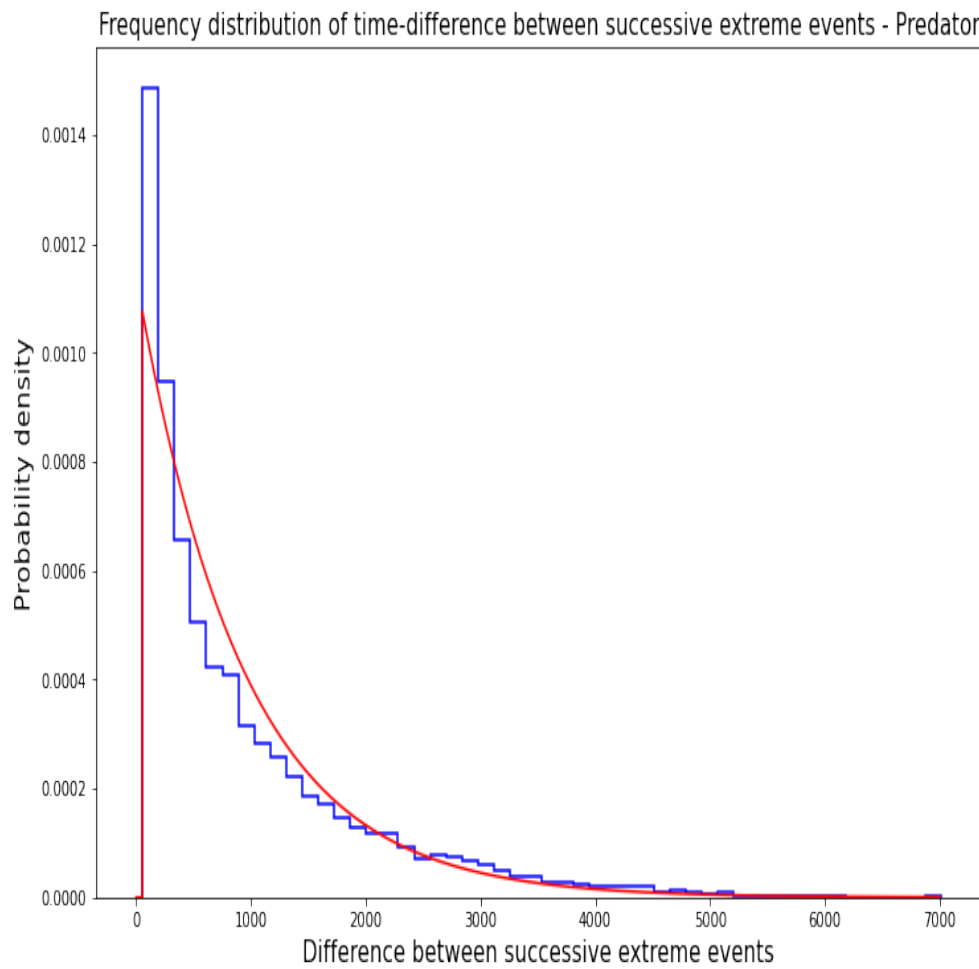


FIGURE 2.11: Probability distribution of the time intervals between two successive extreme events in the predator population- histogram from the raw data and the exponential best fit.

Chapter 3

How extreme are the extreme events?

We have seen the occurrence of extreme events in a ring of coupled systems, each of which on its own exhibits only simple Lotka Volterra dynamics of the generic type. We have seen that in such a ring of coupled systems, each of the individual patches exhibits the occurrence of extreme events in both prey and predator populations, given that we define an event to be ‘extreme’ if the value of the dynamical variable becomes larger than the value ten standard deviations more than the mean value of the dynamical variable. But how extreme are these events? How large does the value of the dynamical variable become when an extreme event happens? Sure, it is more than ten standard deviations away from the mean value (by definition), but how large are these events?

In this chapter we seek answer to such questions. We investigate the actual value of the relevant dynamical variables during the extreme events, and the dependence of the values on various factors.

3.1 A measure for the extremeness of events

We wish to quantify the strength of extreme events in general, given a coupling constant C . There are several ways to do this. We do it in the following way. In our system, there are a total of 100 patches arranged on a ring. As the system evolves in time, the prey and predator populations on each patch evolve. Extreme events do occur on each patch as time goes on (for any small generic values of initial conditions). We let the system evolve in time for a fixed pre-determined duration. After removing the initial transience, we look at the collection of all the local maxima in the time-series that occurred on

all the patches, both in the prey and the predator populations. From the list of all the local maxima in the time series of prey population, we determine the global maximum. We do the same for the predator extreme events. Then we initialize the whole system again with a different randomly chosen set of initial conditions, evolve it again, and again note the globally occurred highest maximum in the whole system for both the prey and the predator. We do this a number of times, save the magnitudes of the global maximum each time. Finally, we compute the arithmetic means of both the lists. (Readers who have read 1 should find this procedure familiar.) Call this mean for the extreme events in prey $\langle v_{max} \rangle$ and the corresponding quantity for the predator $\langle w_{max} \rangle$. We use these two quantities as measures for the strength of extreme events. Note that the averaging is done over different initial conditions, and not over the different patches. We can study the dependence of these quantities on the coupling constant C .

There is one more thing that has to be discussed regarding the evaluation of $\langle v_{max} \rangle$ and $\langle w_{max} \rangle$. When the system is being integrated in time, it might happen that there is a blow-up of one of the variables. We noted that in our system, there are blow-ups in both the prey and predator populations. Note that since there are 100 patches in the ring, even with probabilities as small as $\sim 1/1000$ for a patch to blow up within the time-duration we integrate our system for, the probability that one of the patches will blow up is $\sim 1/10$. But even if one of the 100 patches blows up, it means that the iteration in which this happens is not of any use in the computation of $\langle v_{max} \rangle$ and $\langle w_{max} \rangle$. It should also be noted that the probability of blow-ups increases with the increasing values of the coupling constant C . We have not quantified this, but this was fairly evident when we ran our simulations. Hence, we simply ignored those iterations where any one of the 200 dynamical variables blew up, and started all over again with a different randomly chosen set of initial conditions. This also means that the simulation becomes more and more computationally expensive with increasing values of C .

3.2 Results of simulation

We find the dependence of $\langle v_{max} \rangle$ and $\langle w_{max} \rangle$ on C by performing the integration for different values of C from 0 to 3. The results for $\langle v_{max} \rangle$ and $\langle w_{max} \rangle$ are shown in Figure 3.1 and Figure 3.2 respectively.

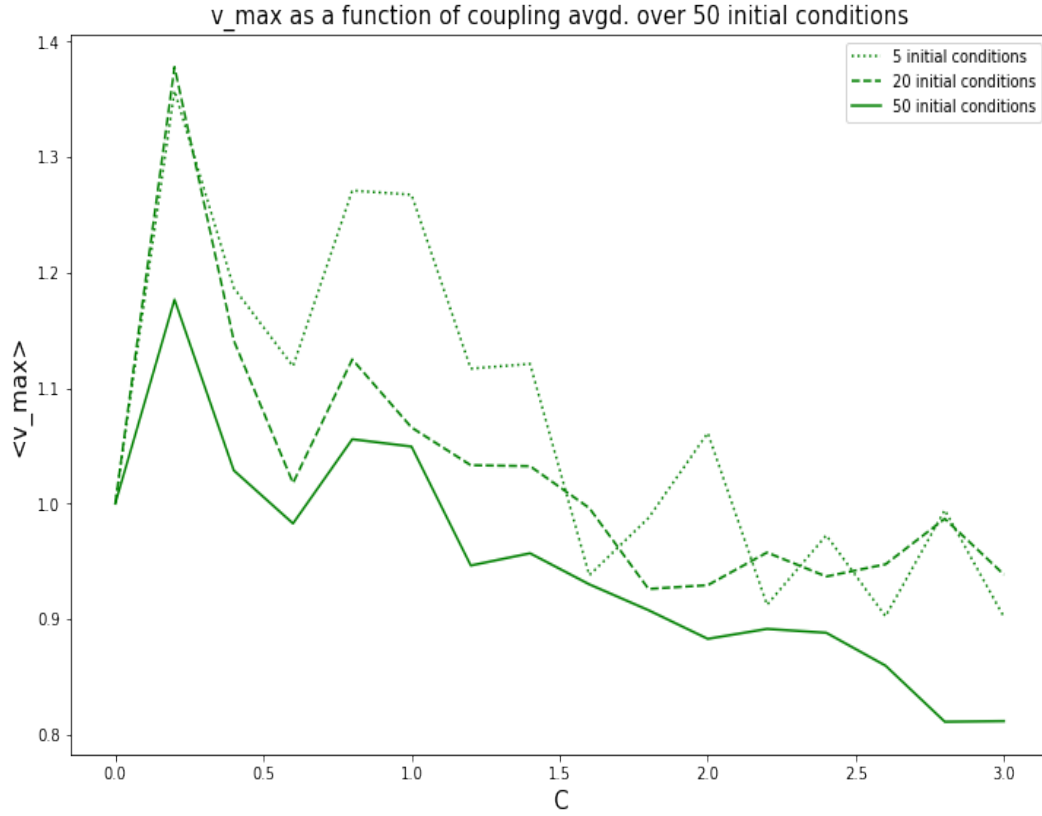


FIGURE 3.1: The dependence of $\langle v_{max} \rangle$ on the coupling constant C for discrete values between 0 and 3, separated by 0.2. The points have been joined. The solid line joins the points obtained when the averaging was performed over 50 initial conditions, and hence is the most reliable. The dashed line joins points that were obtained upon averaging over 20 initial conditions, and the dotted line joins the points that were obtained over 5 initial conditions.

As expected, the pattern becomes more and more smooth with increasing number of iterations of initial conditions over which the averaging is performed. We expect more smoothening can be obtained by increasing the number of initial conditions, obviously it becomes computationally more expensive, and we do not do it any further than averaging over 50 iterations. However, there is another curious trend that is noticeable- the values of either of $\langle v_{max} \rangle$ and $\langle w_{max} \rangle$ in general are smaller if the averaging is over more number of initial conditions. This could be an accident, but seems unlikely. More likely this stems from some underlying reason, something to do with the temporal distribution of maxima, that we don't see yet. Such a feature was also observed in the context of the three-level system we earlier considered. See Chapter 1.

The other general inferences are that for both the predator and the prey, the

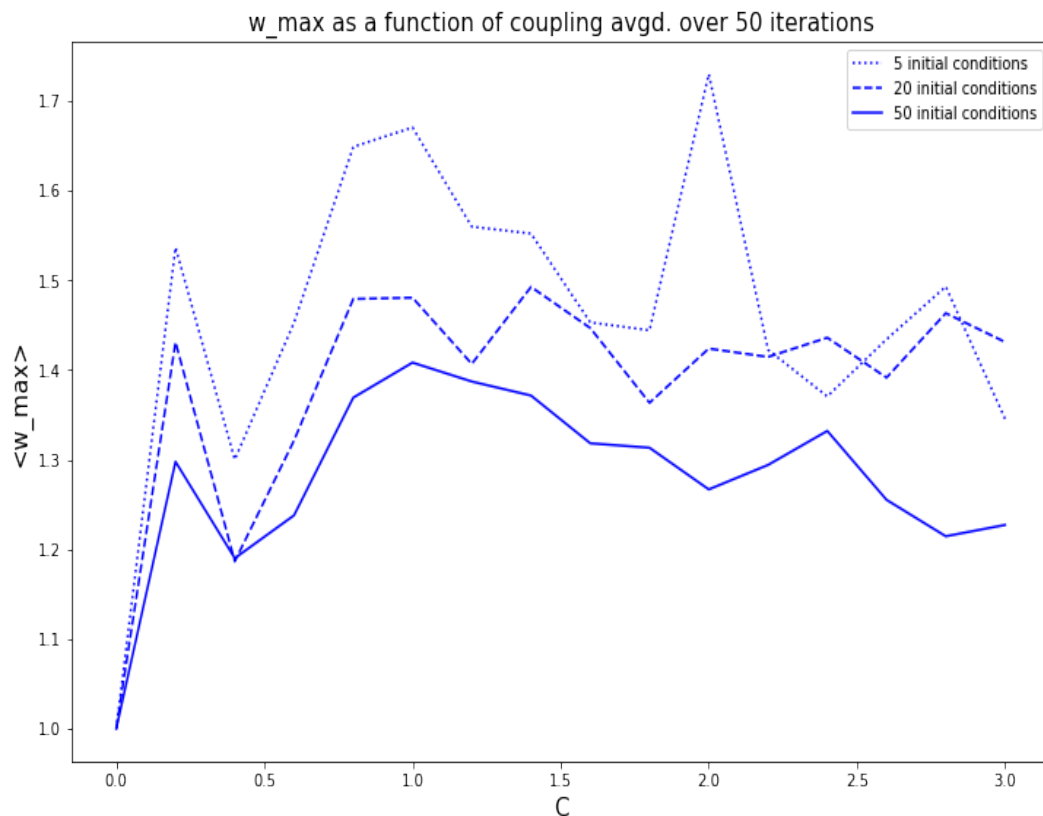


FIGURE 3.2: The dependence of $\langle v_{max} \rangle$ on the coupling constant C for discrete values between 0 and 3, separated by 0.2. The points have been joined. The solid line joins the points obtained when the averaging was performed over 50 initial conditions, and hence is the most reliable. The dashed line joins points that were obtained upon averaging over 20 initial conditions, and the dotted line joins the points that were obtained over 5 initial conditions.

strength of extreme events suddenly rises when C is increased from 0 to around 0.5. Then it suddenly experiences a decrease in strength of C slightly greater than 0.5. Thereafter, the strength of these event decreases steadily for the prey population and remains more or less constant for the predator population, till $C = 3$.

3.3 What is happening for small values of C ?

It can be seen in the Figure 3.1 and Figure 3.2 that the average strength of extreme events is very sensitive to the values of C that are between 0 and 1. For $C = 0$, of course, there are no extreme events. And suddenly for $C \sim 0.5$, the strength of extreme events is very high, while the strength of extreme events again decreases with a slight increase in the value of C from 0.5. However, much cannot be inferred about what is going on in this region when the value of C is between 0 and 1 from Figure 3.1 and Figure 3.2, because our resolution is not that good- there are only 5 values of C between 0 and 1 (both values inclusive) that we have calculated $\langle v_{max} \rangle$ and $\langle w_{max} \rangle$ for.

To see more clearly what is happening for these values of C , we scan this region more closely, with a greater resolution. We calculate $\langle v_{max} \rangle$ and $\langle w_{max} \rangle$ for C between 0 and 1 with a resolution of 0.04. That is, we calculate $\langle v_{max} \rangle$ and $\langle w_{max} \rangle$ for $C = 0, C = 0.04, C = 0.08$, all the way upto $C = 1$. Moreover, we enhance the number of iterations over initial conditions. Figure 3.1 and Figure 3.2 were made with averaging over a maximum of 50 initial conditions. For this plot, we average over 100 initial conditions. This would also confirm our assumption that there is no underlying randomness in what $\langle v_{max} \rangle$ and $\langle w_{max} \rangle$ are for given values of C , and the values can be made more precise by collecting more statistics.

Figure 3.3 and Figure 3.4 show the results of this simulation for the prey and predator populations respectively. First, as expected, the plot is much smoother, owing to greater resolution of sampling, and increasing the number of initial conditions. However, there is a much more striking feature. The curves of $\langle v_{max} \rangle$ and $\langle w_{max} \rangle$ look remarkably similar. There is a very sharp dip in the values of $\langle v_{max} \rangle$ and $\langle w_{max} \rangle$, and this dip occurs for the exactly same value of C for both of them- around $C \sim 0.44$.

We believe this shows that something interesting is going on at $C \sim 0.44$. We investigate the dynamics at this value of C further in the next chapter.

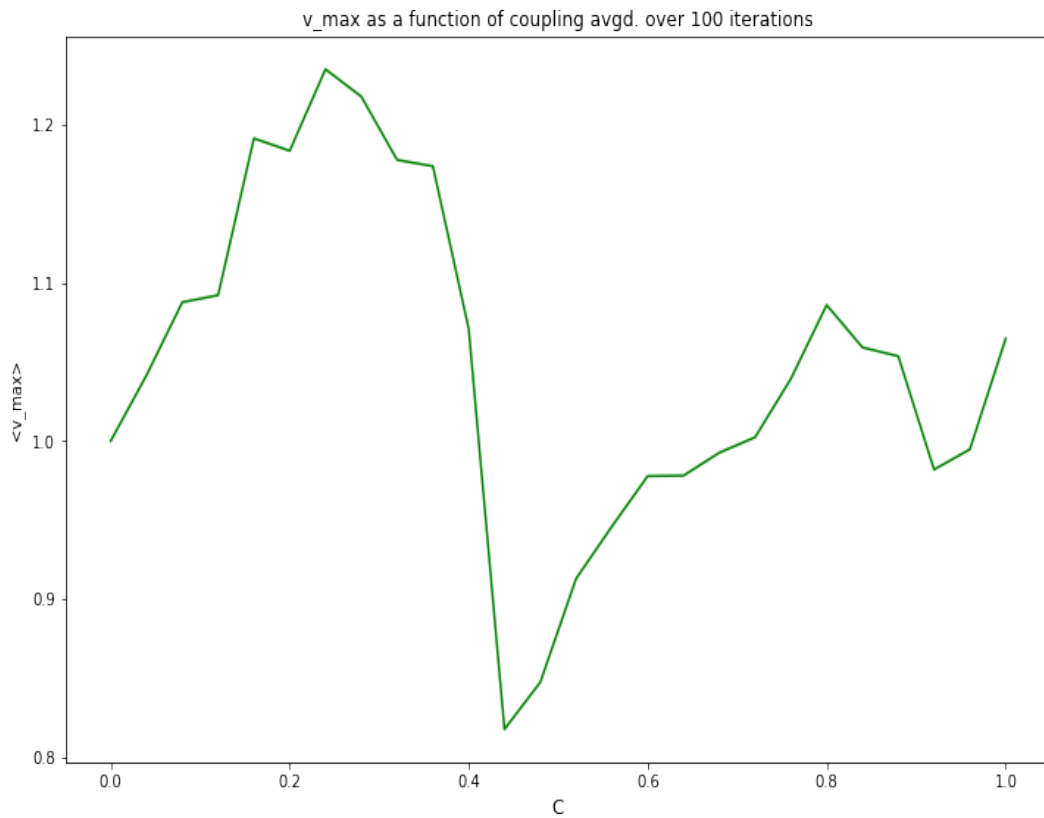


FIGURE 3.3: The dependence of $\langle v_{max} \rangle$ on the coupling constant C for discrete values between 0 and 1, separated by 0.04, averaged over 100 randomized initial conditions. The points have been joined by a line.

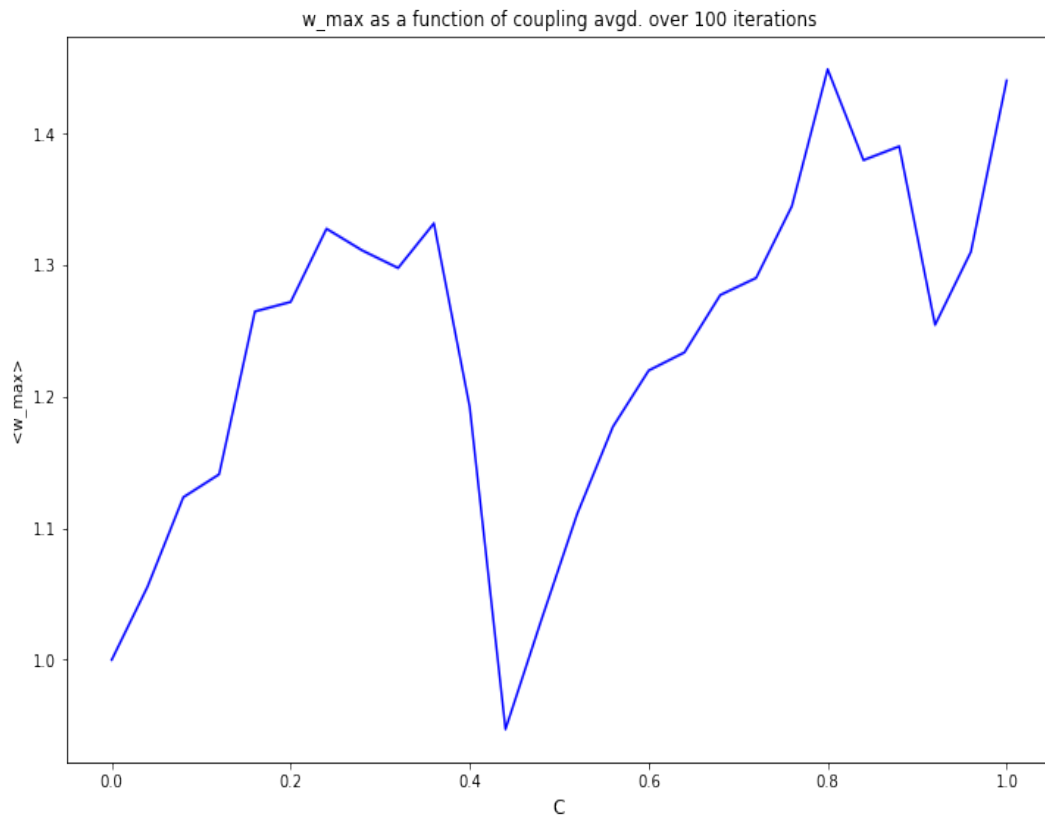


FIGURE 3.4: The dependence of $\langle w_{max} \rangle$ on the coupling constant C for discrete values between 0 and 1, separated by 0.04, averaged over 100 randomized initial conditions. The points have been joined by a line.

Chapter 4

Window of quenched activity

In the previous chapter, we addressed the issue of the strength of extreme events in the system we have been considering. The system consists of ~ 100 coupled islands on a ring, each one exhibiting simple two-level Lotka Volterra dynamics. We defined a measure that quantified for us the strength of extreme events for a given value of C , the coupling constant. We looked at the variation in the strength of extreme events as C as varied, and highlighted some interesting phenomena. One very interesting phenomenon that we noticed was that at $C \sim 0.44$, the strength of extreme events was very low. In fact, the maxima at this value of C could not be called extreme in general. However, there do exist extreme events with a reasonably high frequency for the values of C higher as well as lower than this critical value.

In this chapter, we seek to dig deeper into this phenomenon. We try to characterise this lull in extreme events at $C \sim 0.44$, and look more closely what is happening to the dynamics of the system at the level of each patch, that leads to this extinguishing.

4.1 Bifurcation diagrams

Bifurcation diagrams are used ubiquitously to study the dynamics of dynamical systems that exhibit dynamics in discrete time. A bifurcation diagram [Str18] is a plot that shows the values of a dynamical variable assumed or approached asymptotically, as a function of a parameter of the system. The most popular bifurcation diagram by any account is the one for the popular logistic map [May04]. The map is given by the recursion relation

$$x_{n+1} = rx_n(1 - x_n) \tag{4.1}$$

There is only one dynamical variable x , which evolves in discrete time steps. The value of the dynamical variable at any step is determined by the value at the preceding step in accordance with the equation 4.1. For sufficiently low values of r , the system invariably reaches a stage, where the variable assumes only a small number of values forever again and again. Note that this happens no matter what value of x the system began with. But we can tune r . For different values of r , the system asymptotes to different values of the variable. Hence, we can plot a set of points, with different values of r on the horizontal axis, and the values x will take after some initial transience on the vertical axis. This plot is shown in Figure 4.1.

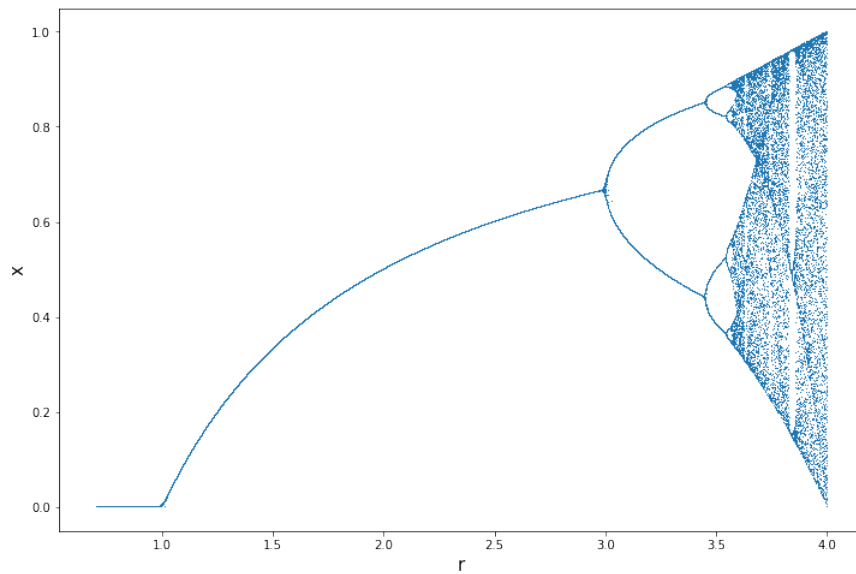


FIGURE 4.1: Bifurcation diagram for the logistic map.

Figure 4.1 is so popular that it has come to be known as the single most image popular image associated to nonlinear dynamics and chaos. It gives a good idea of the dynamics going on for each value of r in the system. This is a general lesson: for a system that has a tunable parameter, the bifurcation diagram gives a general idea of the dynamics happening at each value of the parameter. We have lost the information regarding the temporal changes: there is no time anywhere in the bifurcation diagram, but that is not always required anyway.

Let us now turn back to our system. We intend to study the system for different values of C , and wish to see what is happening at some special value of it, that is, at $C = 0.44$. It should be evident that a bifurcation diagram is the tool that should come handy. However, there is an issue lurking here. The bifurcation diagram, as described above, plotted a finite number of points

for each value of r . A finite number of points are possible for a discrete system. But how do we get a meaningful bifurcation diagram for a system that is evolving continuously in time, like ours? For each value of C , our system's variables are evolving in continuous time. In the next section, we describe how we modify the traditional definition of a bifurcation diagram to suit our problem.

4.2 Bifurcation diagrams for our system

Consider our system defined by equations (2.2). Remember, we are interested in the nature of extreme events in our system, which are very large maximas. Moreover, the feature that we are trying to explain was seen in Figure 3.3 and Figure 3.4. These two figures were made by plotting the local maximas the variables assumed. Hence, it is sensible to focus on maximas only while trying to understand the dynamics of the system- we are principally after the information on the maximas. Hence, we plot an analogue of the bifurcation diagram for our system, that plots the values of the maximas that the dynamical variables the system takes at each value of C . Note that since there are 200 dynamical variables for our system, we can come up with 200 bifurcation diagrams! We can show what values all the v_i 's and the w_i 's take when each of them assume maximas for each value of C . However, it can be expected that only two diagrams corresponding to the two variables on a single patch should give a picture of the dynamics. (We realize later that this expectation is only partly true!)

It should also be borne in mind that we have no a priori reason to expect that the values of maxima for our variables asymptote to any magnitude for any value of C . In fact, we have seen that we usually see a variety of maximas. Hence we do not expect to see any simple features in the diagram for any values of C (except $C = 0$), like Figure 4.1 has for small values of r .

With all this in mind, we set out to get the relevant bifurcation diagrams for our system. We integrate our system, with the values $C = 0$ to $C = 3$ with intervals of 0.02. That is, we integrated the system for $C = 0$, and then for $C = 0.02$, and then for $C = 0.04$, and so on all the way upto $C = 3.0$. We integrate the whole system for 8500 time units for each of these values of C . During each integration, we note down all the maximas that occurred for each of the 200 dynamical variables. (Actually, we picked up the maximas above a very small threshold- 10^{-24}). In the end, we have 200 lists, consisting

of the values of all those maximas that occurred. Finally, to get a meaningful diagram that reflects the general features of dynamics independent of our specific choice of initial conditions, we pick up only the later 15000 maximas (total number of maximas was of the order of 20000) in each of the lists, leaving out the rest as transience.

We finally have the data points, ready to be plotted and turned into a bifurcation diagram. Let's see what those plots look like.

Figure 4.2 shows the bifurcation diagram for a representative patch's prey and Figure 4.3 shows the bifurcation diagram for that same patch's predator.

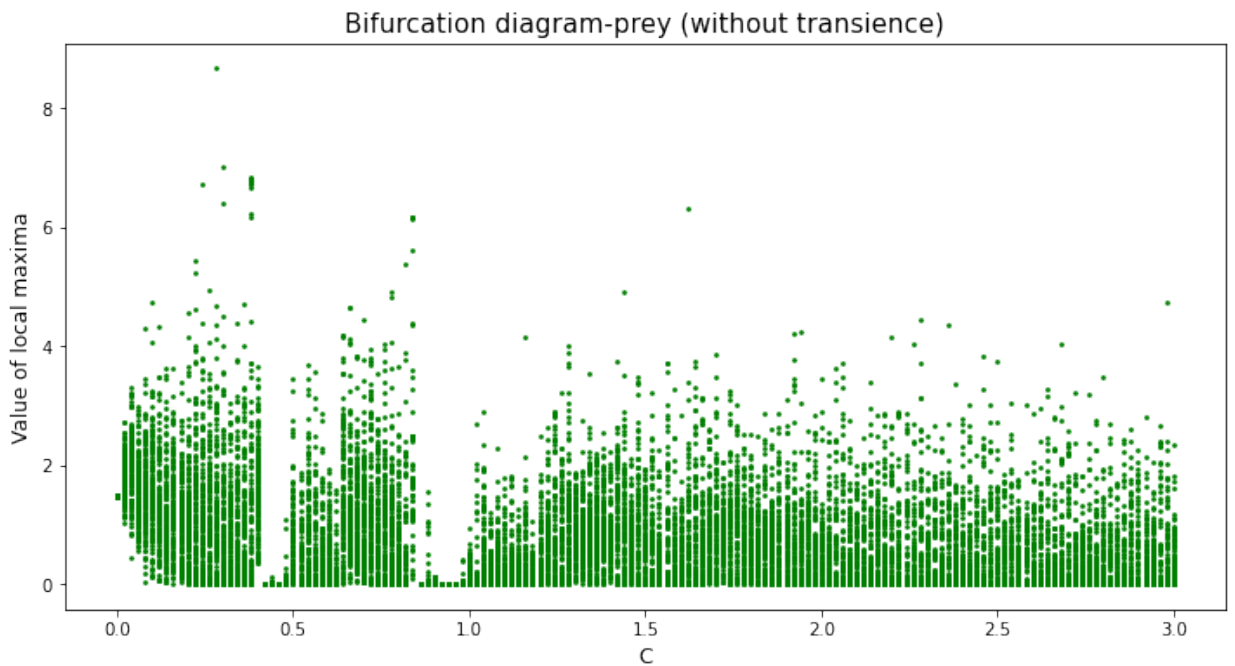


FIGURE 4.2: Bifurcation diagram comprising of all the local maximas as coupling is varied, for prey.

We notice that there is a window of inactivity at around $C \sim 0.44$ in Figure 4.2. This is according to our expectations. But it is surprising that there is no such corresponding window of activity at this value of C in Figure 4.3, the bifurcation diagram for the predator on the same patch. We saw, however, in the previous chapter, that the decrease in the strength of extreme events for this value of C happened for both the prey and the predator.

It should also be noted that there is another window of activity at around $C \sim 0.9$, again only in the bifurcation diagram of prey.

To see why the window of activity appears only for the prey and not for the predator, it is perhaps instructive to do make the same diagrams again,

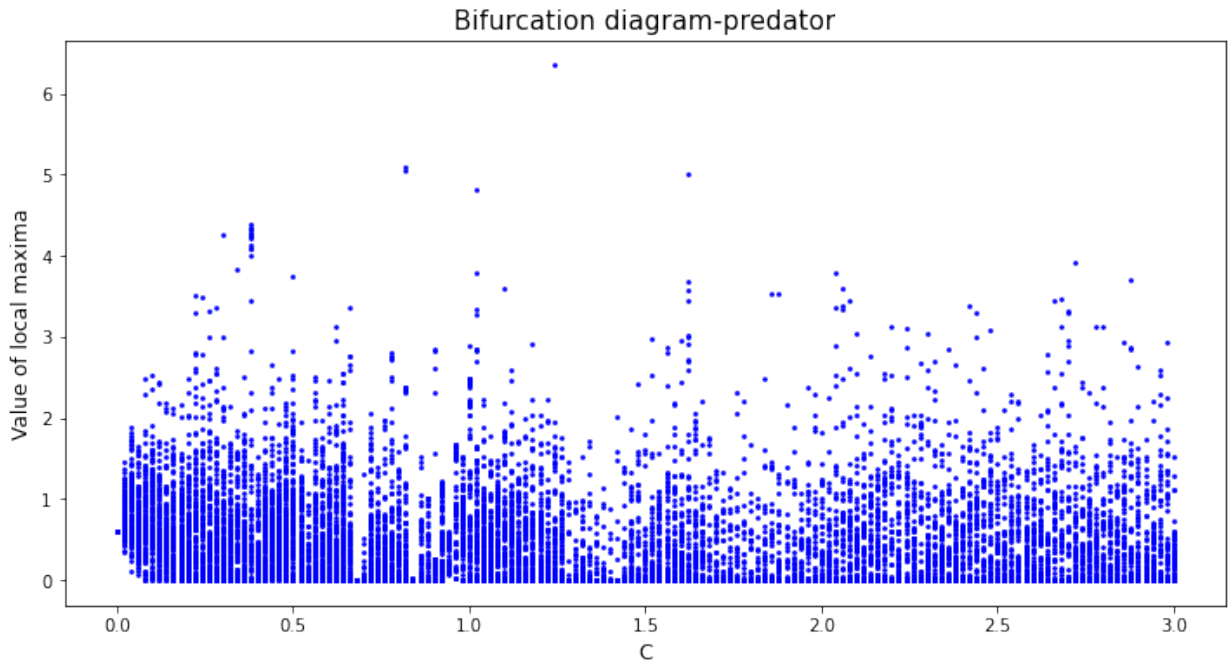


FIGURE 4.3: Bifurcation diagram comprising of all the local maximas as coupling is varied, for predator.

with a different set of random initial conditions. We follow the exact same procedure as was followed in making Figures 4.2 and (4.3), and get two more bifurcation diagrams.

Figures 4.4 and 4.5 show the bifurcation diagrams made such.

In the bifurcation diagram for the predator (Figure 4.5), one sees that one can see the window of inactivity at $C \sim 0.44$. But there seems to be no window of inactivity in the bifurcation diagram of prey (Figure 4.4)! Also, just like in Figure 4.2, there is also a window of inactivity at $C \sim 0.9$ in addition to the expected inactivity at $C \sim 0.44$.

A few more times trying to get the window of inactivity in the both diagrams- the one for prey and the one for predator by us goes in vain.

4.3 Mass-extinctions brought about by coupling

To actually see what is happening that we either see a window of activity in the bifurcation diagram of prey only or that of predator only, but the dip in extreme events is so similar in both the cases if we set $C \sim 0.44$, we plot the time-series of both the prey and predator for two representative patches at $C \sim 0.44$.

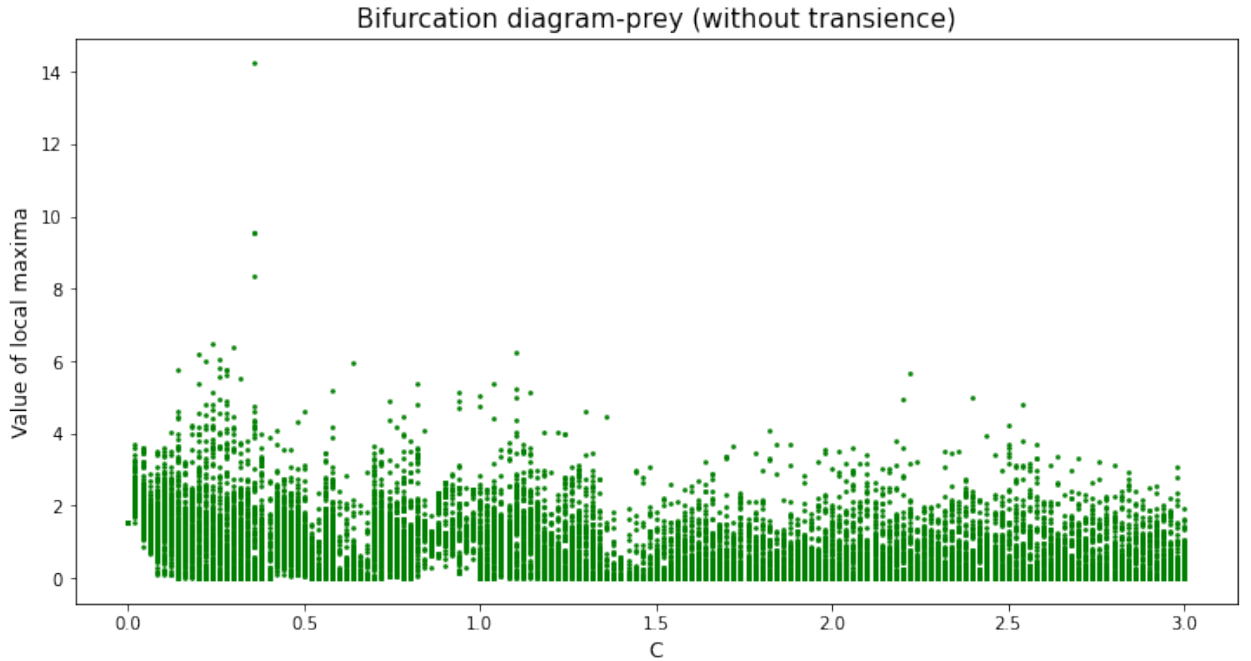


FIGURE 4.4: Bifurcation diagram comprising of all the local maximas as coupling is varied, for prey.

Note that in the two cases we have shown, either the prey goes extinct on a patch or the predator. Repeated trials show that this is a very general trend at $C \sim 0.44$. It happens extremely often that on a patch one of the two species goes extinct. That is why the bifurcation diagrams above showed the window of inactivity only in either the prey or the predator. The window of inactivity appeared in the bifurcation diagram of whichever species happened to go extinct on that particular patch, while the other species did not go extinct, and its population exhibited a behaviour as shown in the above figures, and hence no window of activity was seen in its bifurcation diagram. However, the Figures 3.3 and 3.4 were made after taking average over many many patches over many iterations. Hence, both of them show a remarkably similar decrease in the strength of extreme events.

Note that there is a general lesson we have to take here- that just the right amount of coupling in Lotka Volterra systems can induce mass-extinctions. The general explanation of why there be no widespread extinctions for C less than 0.44 and also for C greater than 0.44, while being present for $C = 0.4$ is at the moment unknown to the authors.

The spatial distribution of these extinctions in the ring of 100 patches deserves some discussion. It is generally seen that extinctions tend to happen

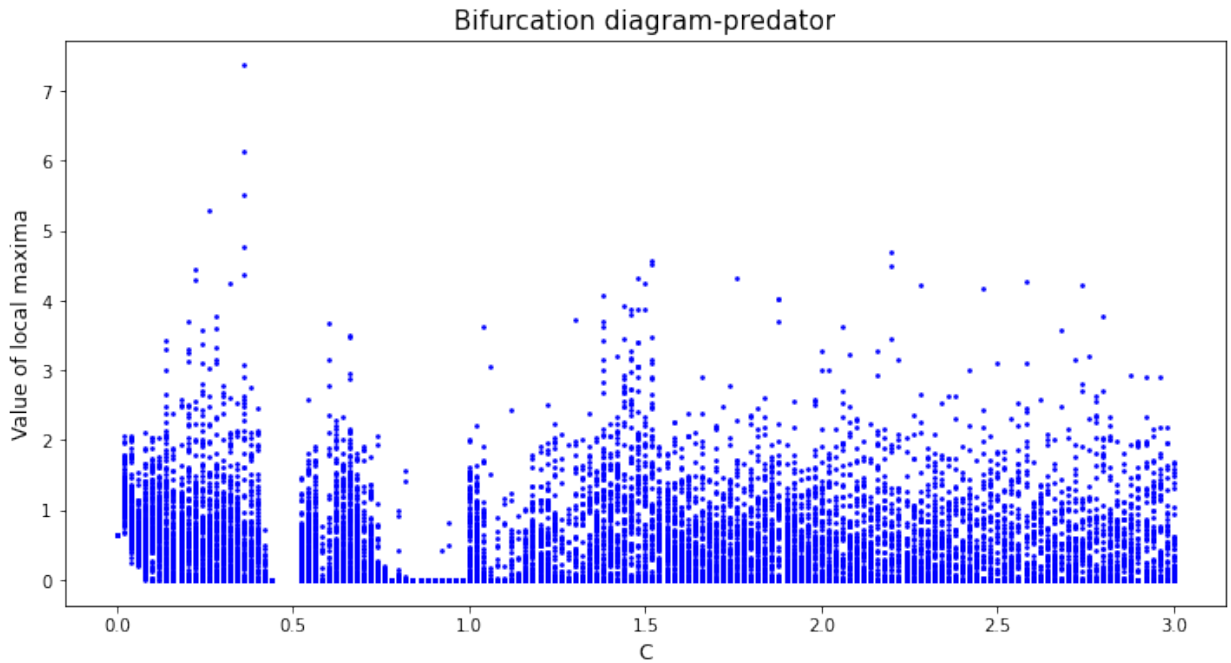


FIGURE 4.5: Bifurcation diagram comprising of all the local maximas as coupling is varied, for predator.

alternately- the patches were the prey and the predator alternate tend to alternate in the ring. Also, there are some patches where none of the prey or the predator go extinct. Such patches tend to exist in clusters in the ring.

We show in Figure 4.8 a schematic of the ring of 100 patches that are integrated for 8000 time units, with a $C = 0.44$. The patches have been colour coded according to their status of extinction at that instant.

We also mention in passing something about the window of inactivity that is seen in Figures 4.2 and 4.5 at $C \sim 0.9$. Upon looking at the time series of various patches when the system is integrated at this value of C , it turns out that the underlying cause for the suppression of extreme events in this window is also mass extinctions of both the species. This dynamics in this window is quite similar to the one at $C \sim 0.44$.

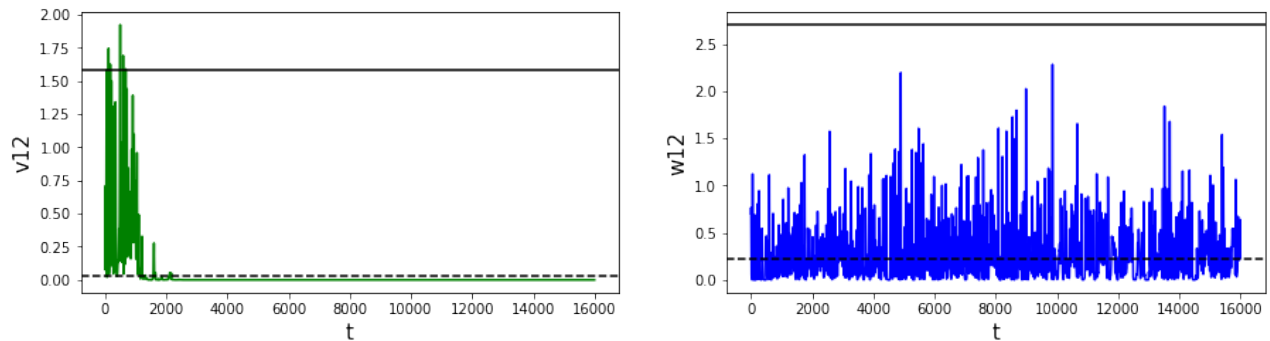


FIGURE 4.6: Time-series for a representative patch at $C \sim 0.44$. Note that the prey gets extinct fairly quickly and the predator population sees a continuous series of spurts. However, these spurts are relatively smaller and none of these are extreme events according to our definition.

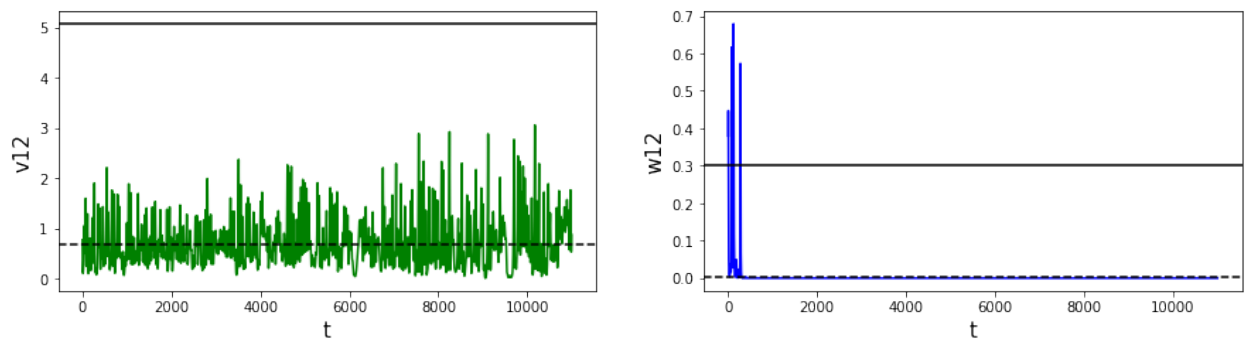


FIGURE 4.7: Time-series for a representative patch at $C \sim 0.44$. Note that the predator gets extinct fairly quickly and the prey population sees a continuous series of spurts. However, these spurts are relatively smaller and none of these are extreme events according to our definition.

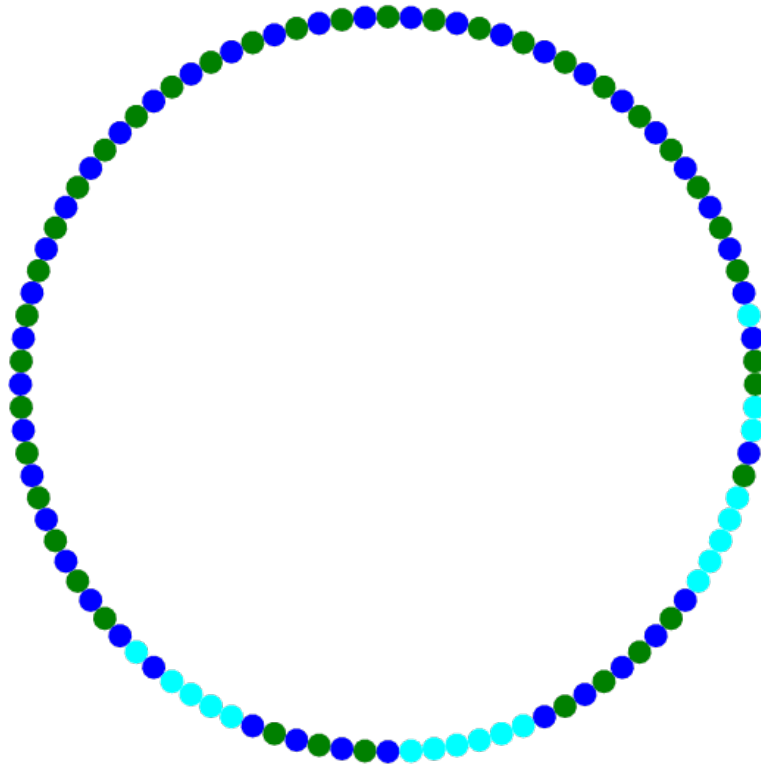


FIGURE 4.8: The extinction of either of the species on the 100 patches- at a representative instant of time after transience. **Blue** patches represent patches which have only the predator present, which means, the prey has gone extinct. **Green** patches represent those where only the prey survives, and hence the predator has gone extinct. **Aqua** circles represent the patches on which neither has gone extinct.

Bibliography

- [AJK06] Sergio Albeverio, Volker Jentsch, and Holger Kantz. *Extreme events in nature and society*. Springer Science & Business Media, 2006.
- [BHS99] Bernd Blasius, Amit Huppert, and Lewi Stone. “Complex dynamics and phase synchronization in spatially extended ecological systems”. In: *Nature* 399.6734 (1999), pp. 354–359.
- [CVS20] Sudhanshu Shekhar Chaurasia, Umesh Kumar Verma, and Sudeshna Sinha. “Advent of extreme events in predator populations”. In: *Scientific Reports* 10.1 (2020), pp. 1–10.
- [May04] Robert M May. “Simple mathematical models with very complicated dynamics”. In: *The Theory of Chaotic Attractors* (2004), pp. 85–93.
- [Str18] Steven H Strogatz. *Nonlinear dynamics and chaos with student solutions manual: With applications to physics, biology, chemistry, and engineering*. CRC press, 2018.